HETEROGENEOUS SHALLOW-SHELF CARBONATE BUILDUPS IN THE PARADOX BASIN, UTAH AND COLORADO: TARGETS FOR INCREASED OIL PRODUCTION AND RESERVES USING HORIZONTAL DRILLING TECHNIQUES

(Contract No. DE-2600BC15128)

DELIVERABLE 1.2.6
THIN SECTION CATHODOLUMINESCENCE: CHEROKEE AND BUG FIELDS, SAN JUAN COUNTY, UTAH

Submitted by

Utah Geological Survey
Salt Lake City, Utah 84114
April 2005

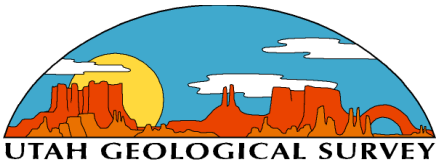

Contracting Officer's Representative

Virginia Weyland, Contract Manager
U.S. Department of Energy
National Petroleum Technology Office
1 West 3rd Street
Tulsa, OK 74103-3532

DISCLAIMER

This report was prepared as an account of work sponsored by an agency of the United States Government. Neither the United States Government nor any agency thereof, nor any of their employees, makes any warranty, express or implied, or assumes any legal liability or responsibility for the accuracy, completeness, or usefulness of any information, apparatus, product, or process disclosed, or represents that its use would not infringe privately owned rights. Reference herein to any specific commercial product, process, or service by trade name, trademark, manufacturer, or otherwise does not necessarily constitute or imply its endorsement, recommendation, or favoring by the United States Government or any agency thereof. The views and opinions of authors expressed herein do not necessarily state or reflect those of the United States Government or any agency thereof.

Although this product represents the work of professional scientists, the Utah Department of Natural Resources, Utah Geological Survey, makes no warranty, express or implied, regarding its suitability for a particular use. The Utah Department of Natural Resources, Utah Geological Survey, shall not be liable under any circumstances for any direct, indirect, special, incidental, or consequential damages with respect to claims by users of this product.

HETEROGENEOUS SHALLOW-SHELF CARBONATE BUILDUPS IN THE PARADOX BASIN, UTAH AND COLORADO: TARGETS FOR INCREASED OIL PRODUCTION AND RESERVES USING HORIZONTAL DRILLING TECHNIQUES

(Contract No. DE-2600BC15128)

DELIVERABLE 1.2.6
THIN SECTION CATHODOLUMINESCENCE: CHEROKEE AND BUG FIELDS, SAN JUAN COUNTY, UTAH

Submitted by

Utah Geological Survey
Salt Lake City, Utah 84114
April 2005

by

David E. Eby, Eby Petrography & Consulting, Inc.
and
Thomas C. Chidsey, Jr., Principal Investigator/Program Manager,
and Craig D. Morgan
Utah Geological Survey

CONTENTS

FIGURES

TABLES

INTRODUCTION

Over 400 million barrels (64 million m^3) of oil have been produced from the shallow-shelf carbonate reservoirs in the Pennsylvanian (Desmoinesian) Paradox Formation in the Paradox Basin, Utah and Colorado. With the exception of the giant Greater Aneth field, the other 100 plus oil fields in the basin typically contain 2 to 10 million barrels (0.3-1.6 million m^3) of original oil in place. Most of these fields are characterized by high initial production rates followed by a very short productive life (primary), and hence premature abandonment. Only 15 to 25 percent of the original oil in place is recoverable during primary production from conventional vertical wells.

An extensive and successful horizontal drilling program has been conducted in the giant Greater Aneth field. However, to date, only two horizontal wells have been drilled in small Ismay and Desert Creek fields. The results from these wells were disappointing due to poor understanding of the carbonate facies and diagenetic fabrics that create reservoir heterogeneity. These small fields, and similar fields in the basin, are at high risk of premature abandonment. At least 200 million barrels (31.8 million m^3) of oil will be left behind in these small fields because current development practices leave compartments of the heterogeneous reservoirs undrained. Through proper geological evaluation of the reservoirs, production may be increased by 20 to 50 percent through the drilling of low-cost single or multilateral horizontal legs from existing vertical development wells. In addition, horizontal drilling from existing wells minimizes surface disturbances and costs for field development, particularly in the environmentally sensitive areas of southeastern Utah and southwestern Colorado.

GEOLOGIC SETTING

The Paradox Basin is located mainly in southeastern Utah and southwestern Colorado with a small portion in northeastern Arizona and the northwestern most corner of New Mexico (figure 1). The Paradox Basin is an elongate, northwest-southeast trending evaporitic basin that predominately developed during the Pennsylvanian (Desmoinesian), about 330 to 310 million years ago (Ma). During the Pennsylvanian, a pattern of basins and fault-bounded uplifts developed from Utah to Oklahoma as a result of the collision of South America, Africa, and southeastern North America (Kluth and Coney, 1981; Kluth, 1986), or from a smaller scale collision of a microcontinent with south-central North America (Harry and Mickus, 1998). One result of this tectonic event was the uplift of the Ancestral Rockies in the western United States. The Uncompahgre Highlands in eastern Utah and western Colorado initially formed as the westernmost range of the Ancestral Rockies during this ancient mountain-building period. The Uncompahgre Highlands (uplift) is bounded along the southwestern flank by a large basement-involved, high-angle reverse fault identified from geophysical seismic surveys and exploration drilling. As the highlands rose, an accompanying depression, or foreland basin, formed to the southwest — the Paradox Basin. Rapid subsidence, particularly during the Pennsylvanian and then continuing into the Permian, accommodated large volumes of evaporitic and marine sediments that intertongue with non-marine arkosic material shed from the highland area to the northeast (Hintze, 1993). The Paradox Basin is surrounded by other uplifts and basins that formed during the Late Cretaceous-early Tertiary Laramide orogeny (figure 1).

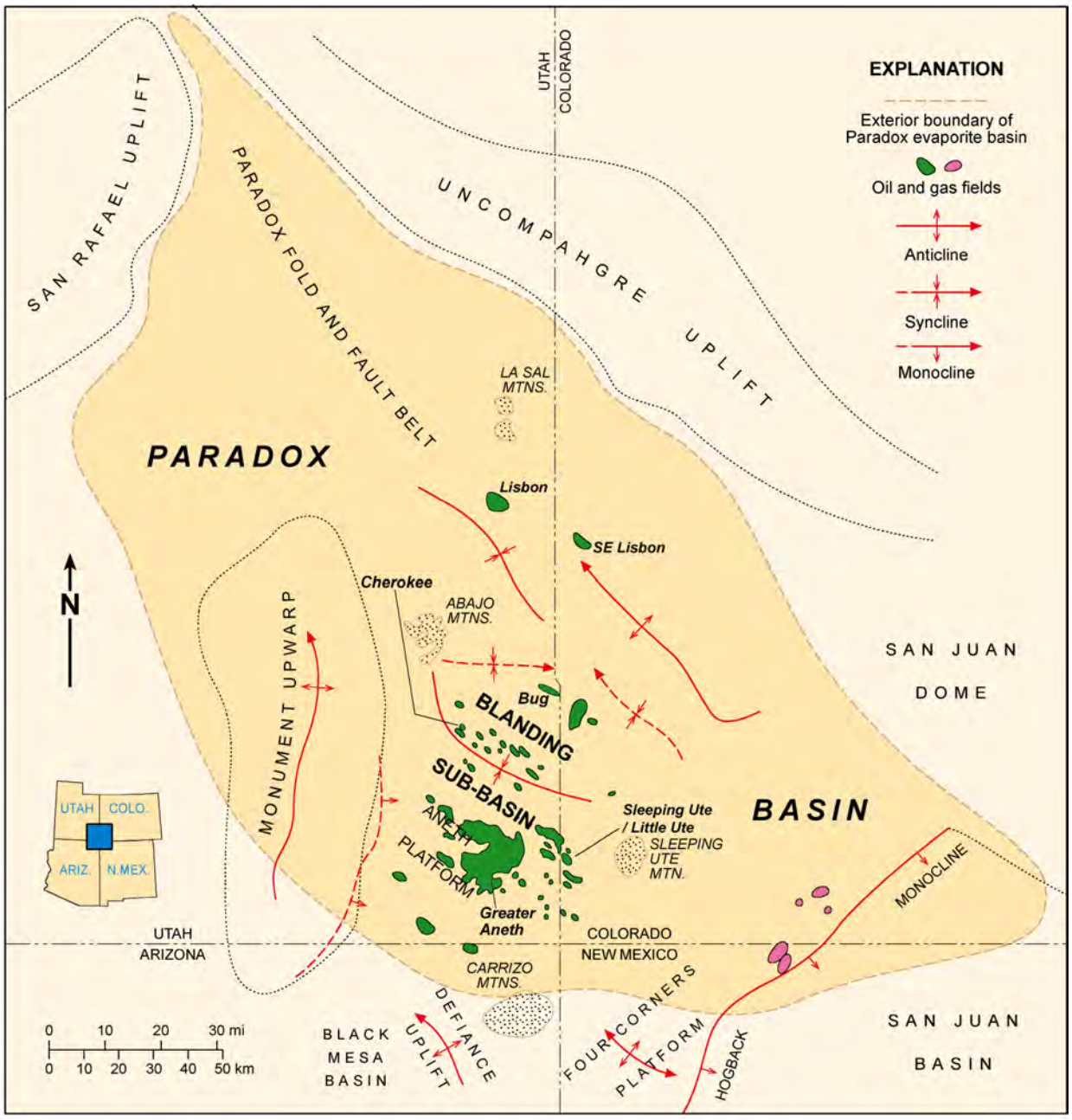

Figure 1. Location map of the Paradox Basin, Utah, Colorado, Arizona, and New Mexico showing producing oil and gas fields, the Paradox fold and fault belt, and Blanding sub-basin as well as surrounding Laramide basins and uplifts (modified from Harr, 1996).

The Paradox Basin can generally be divided into two areas: the Paradox fold and fault belt in the north, and the Blanding sub-basin in the south-southwest (figure 1). Most oil production comes from the Blanding sub-basin. The source of the oil is several black, organic-rich shales within the Paradox Formation (Hite and others, 1984; Nuccio and Condon, 1996). The relatively undeformed Blanding sub-basin developed on a shallow-marine shelf which locally contained algal-mound and other carbonate buildups in a subtropical climate.

The two main producing zones of the Paradox Formation are informally named the Ismay and the Desert Creek (figure 2). The Ismay zone is dominantly limestone comprising equant buildups of phylloid-algal material with locally variable small-scale subfacies (figure 3A) and capped by anhydrite. The Ismay produces oil from fields in the southern Blanding sub-basin (figure 4). The Desert Creek zone is dominantly dolomite comprising regional nearshore shoreline trends with highly aligned, linear facies tracts (figure 3B). The Desert Creek produces oil in fields in the central Blanding sub-basin (figure 4). Both the Ismay and Desert Creek buildups generally trend northwest-southeast. Various facies changes and extensive diagenesis have created complex reservoir heterogeneity within these two diverse zones.

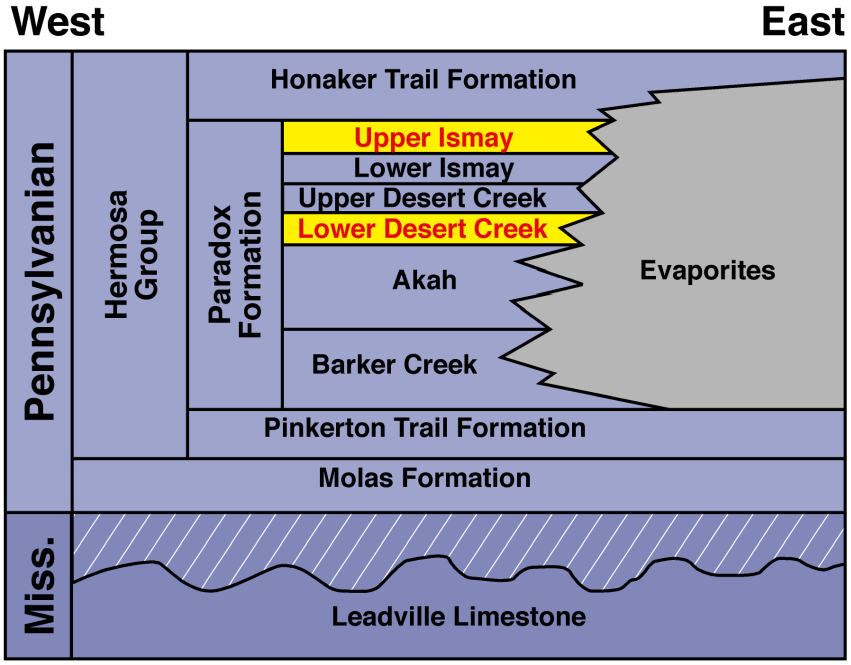

Figure 2. Pennsylvanian stratigraphy of the southern Paradox Basin including informal zones of the Paradox Formation; the Ismay and Desert Creek zones productive in the case-study fields described in this report are highlighted.

CASE-STUDY FIELDS

Two Utah fields were selected for local-scale evaluation and geological characterization: Cherokee in the Ismay trend and Bug in the Desert Creek trend (figure 4). The diagenetic evaluation summarized in this report included cathodoluminescence (CL) examination, photomicroscopy, description, and interpretation of thin section samples from these fields.

This geological characterization focused on reservoir diagenesis, heterogeneity, quality, and lateral continuity, as well as possible compartmentalization within the fields. From these evaluations, untested or under-produced compartments can be identified as targets for horizontal drilling. The models resulting from the geological and reservoir characterization of these fields can be applied to similar fields in the basin (and other basins as well) where data might be limited.

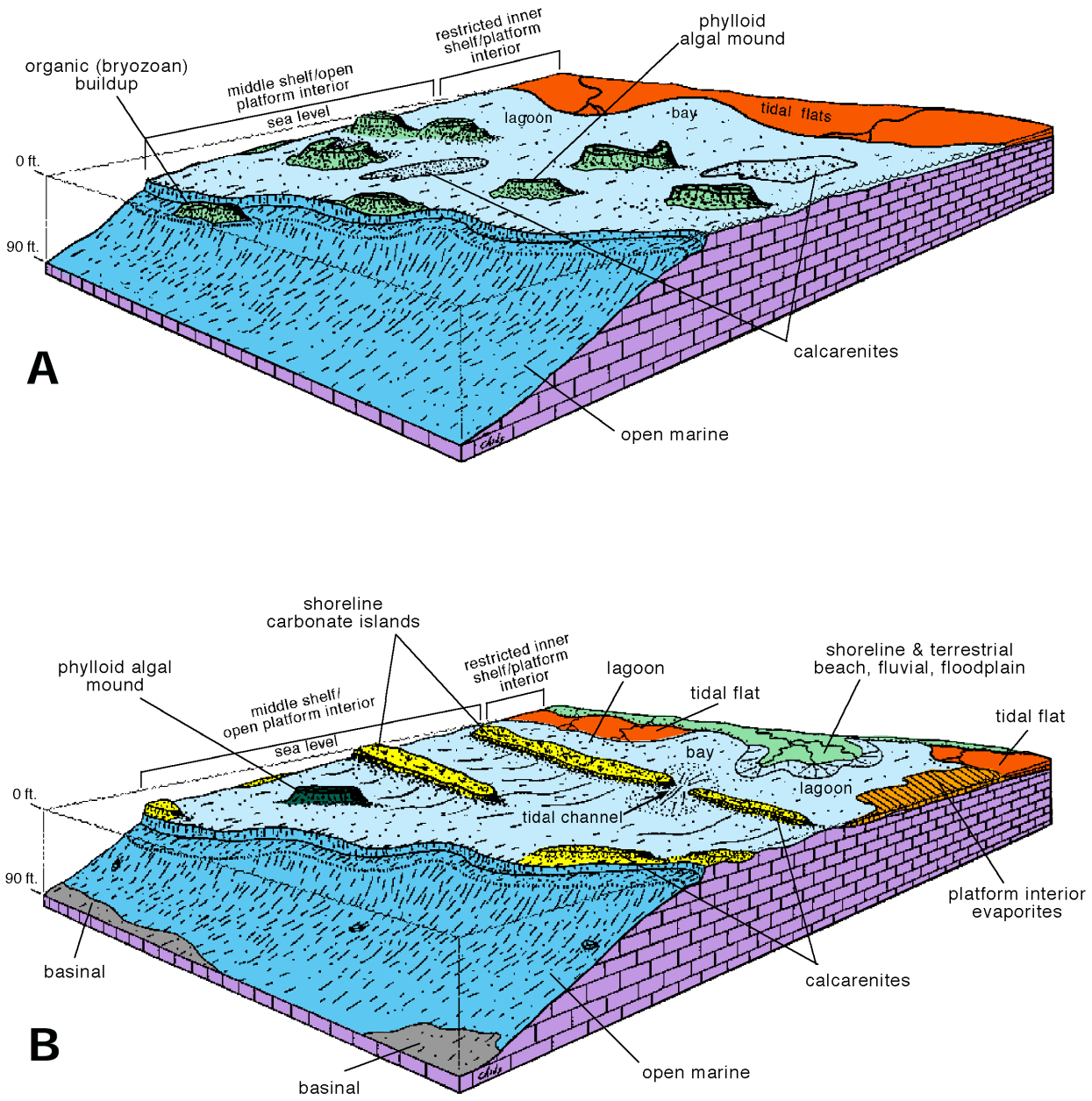

Figure 3. Block diagrams displaying major depositional facies, as determined from core, for the Ismay (A) and Desert Creek (B) zones, Pennsylvanian Paradox Formation, Utah and Colorado.

Cherokee Field

Cherokee field (figure 4) is a phylloid-algal buildup capped by anhydrite that produces from porous algal limestone and dolomite in the upper Ismay zone. The net reservoir thickness is 27 feet (8.2 m), which extends over a 320-acre (130 ha) area. Porosity averages 12 percent with 8 millidarcies (md) of permeability in vuggy and intercrystalline pore systems. Water saturation is 38.1 percent (Crawley-Stewart and Riley, 1993).

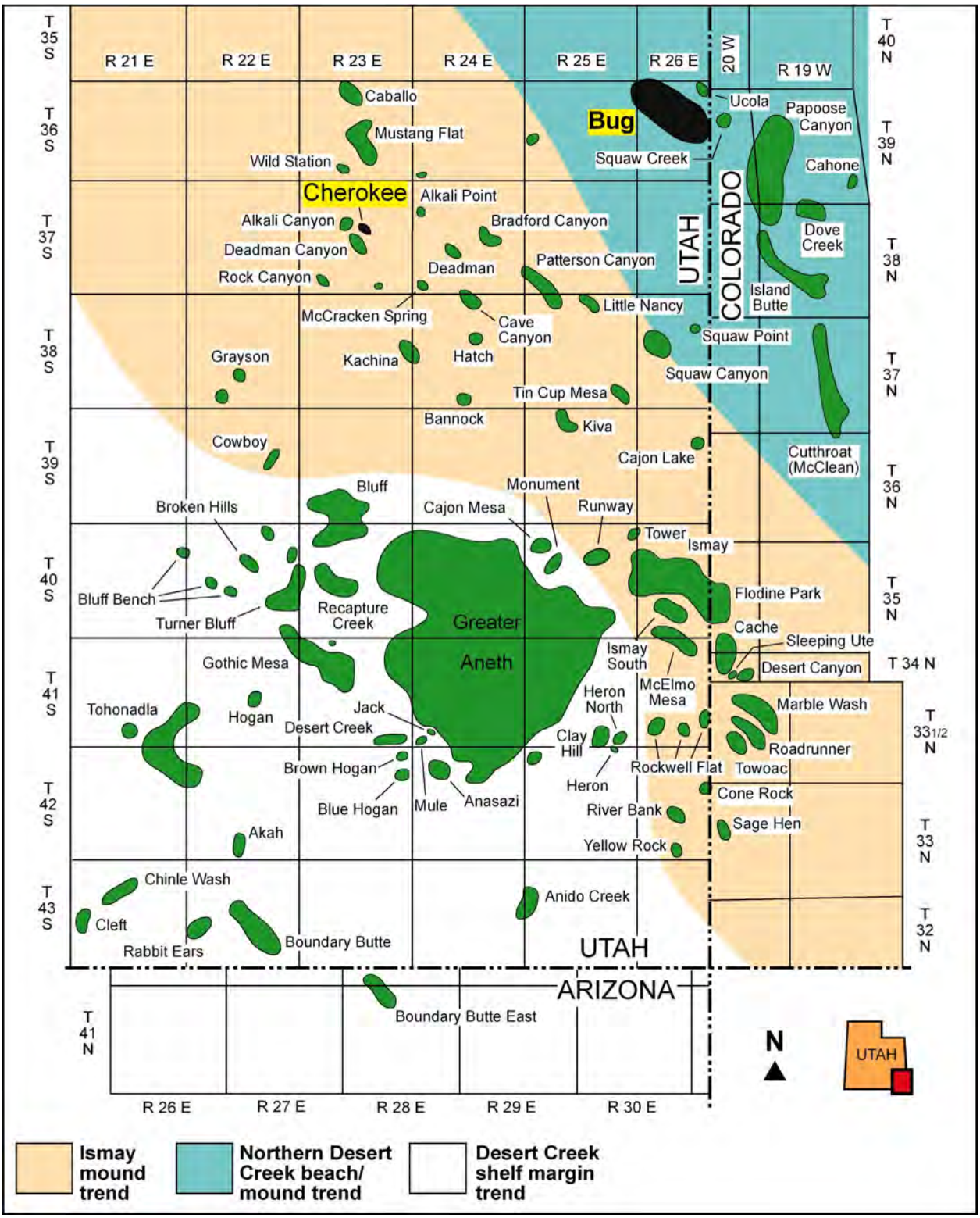

Figure 4. Map showing the project study area and fields (case-study fields in black) within the Ismay and Desert Creek producing trends in the Blanding sub-basin, Utah and Colorado.

Cherokee field was discovered in 1987 with the completion of the Meridian Oil Company Cherokee Federal 11-14, NE1/4NW1/4 section 14, T. 37 S., R. 23 E., Salt Lake Base Line and Meridian (SLBL&M); initial flowing potential (IFP) was 53 barrels of oil per day (BOPD) (8.4 m^3), 990 thousand cubic feet of gas per day (MCFGPD) (28 MCMPD), and 26 barrels of water (4.1 m^3). There are currently four producing (or shut-in) wells and two dry holes in the field. The well spacing is 80 acres (32 ha). The present field reservoir pressure is estimated at 150 pounds per square inch (psi) (1034 Kpa). Cumulative production as of December 1, 2004, was 182,901 barrels of oil (29,081 m^3), 3.68 billion cubic feet of gas (BCFG) (0.1 BCMG), and 3358 barrels of water (534 m^3) (Utah Division of Oil, Gas and Mining, 2004). The original estimated primary recovery is 172,000 barrels of oil (27,348 m^3) and 3.28 BCFG (0.09 BCMG) (Crawley-Stewart and Riley, 1993). The fact that both these estimates have been surpassed suggests significant additional reserves could remain.

Bug Field

Bug field (figure 4) is an elongate, northwest-trending carbonate buildup in the lower Desert Creek zone. The producing units vary from porous dolomitized bafflestone to packstone and wackestone. The trapping mechanism is an updip porosity pinchout. The net reservoir thickness is 15 feet (4.6 m) over a 2600-acre (1052 ha) area. Porosity averages 11 percent in moldic, vuggy, and intercrystalline networks. Permeability averages 25 to 30 md, but ranges from less than 1 to 500 md. Water saturation is 32 percent (Martin, 1983; Oline, 1996).

Bug field was discovered in 1980 with the completion of the Wexpro Bug No. 1, NE1/SE1/4 section 12, T. 36 S., R. 25 E., SLBL&M, for an IFP of 608 BOPD (96.7 m^3), 1128 MCFGPD (32 MCMPD), and 180 barrels of water (28.6 m^3). There are currently eight producing (or shut-in) wells, five abandoned producers, and two dry holes in the field. The well spacing is 160 acres (65 ha). The present reservoir field pressure is 3550 psi (24,477 Kpa). Cumulative production as of December 1, 2004, was 1,622,863 barrels of oil (258,035 m^3), 4.49 BCFG (0.13 BCMG), and 3,181,467 barrels of water (505,853 m^3) (Utah Division of Oil, Gas and Mining, 2004). Estimated primary recovery is 1,600,000 bbls (254,400 m^3) of oil and 4 BCFG (0.1 BCMG) (Oline, 1996). Again, since the original reserve estimates have been surpassed and the field is still producing, significant additional reserves likely remain.

CATHODOLUMINESCENCE

Introduction

Cathodoluminescence is the emission of light resulting from the bombardment of materials using a cathode ray (Allan and Wiggins, 1993). This petrographic technique can be an invaluable tool in petrographic studies of carbonate rocks. This technique can provide important information about the complex modification of rock fabrics and porosity within the lower Desert Creek and upper Ismay zones of the Blanding sub-basin. Diagenesis played a major role in the development of reservoir heterogeneity in Bug and Cherokee fields as well as throughout the all of the Paradox Formation fields. Diagenetic processes started during deposition and continued throughout burial history (figure 5). A complete discussion on the diagenetic history based upon visual core examination and thin section petrography was

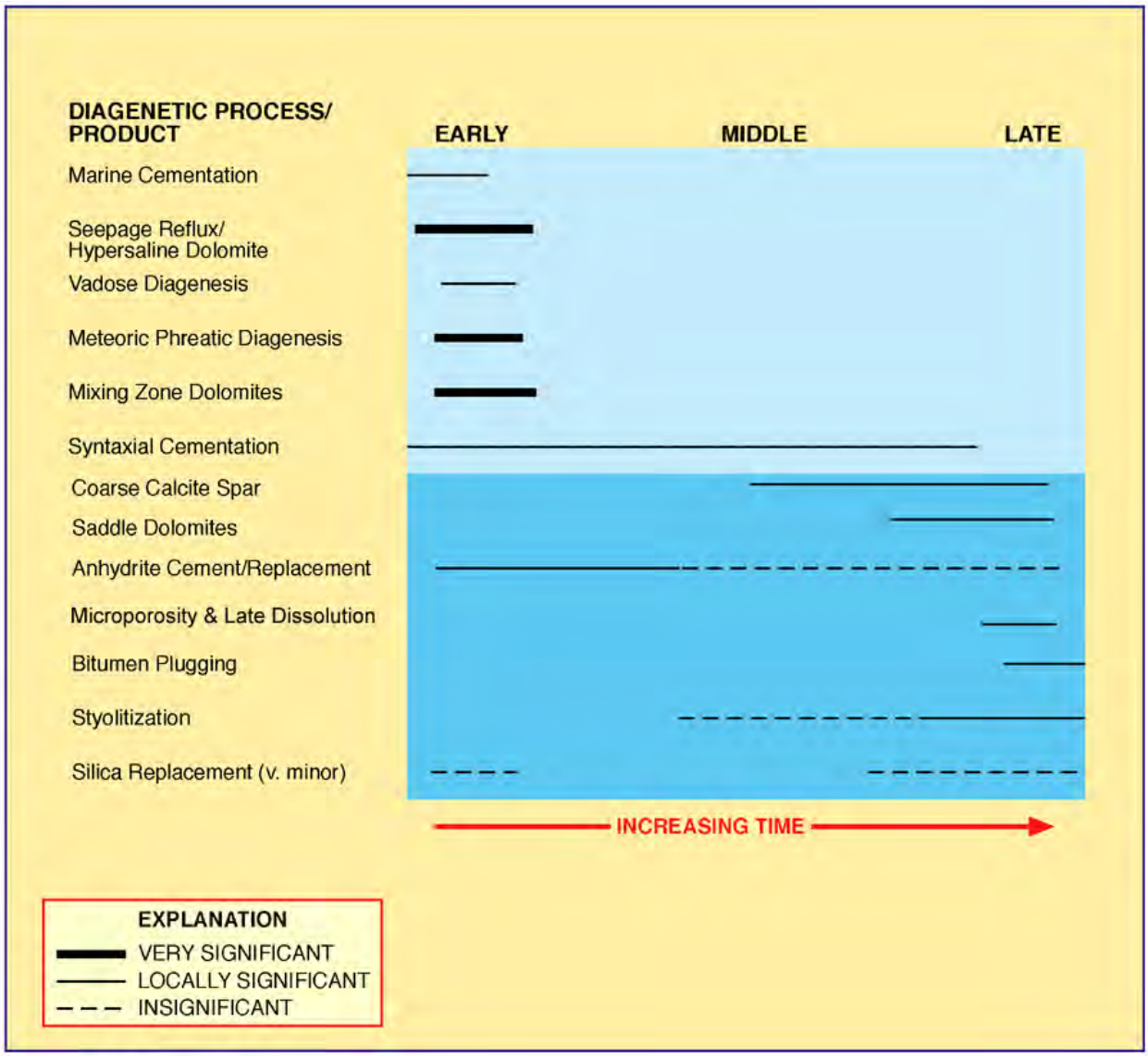

Figure 5. Ideal diagenetic sequence through time based on thin section analysis, Ismay and Desert Creek zones, Cherokee and Bug fields.

documented previously in **Deliverable 1.2.1A – Thin Section Descriptions: Cherokee and Bug Fields, San Juan County, Utah.**

Cathodoluminescence has been used in recent years to provide insights into the chemical differences between preserved remnants of depositional components resulting from various diagenetic events in carbonate rocks as recognized from core examination and thin section petrography. In particular, CL provides visual information on the spatial distribution of certain trace elements, especially manganese (Mn^{2+}) and iron (Fe^{2+}) in calcites and dolomites (Machel and Burton, 1991; Scholle and Ulmer-Scholle, 2003). The visible CL responses are red to orange in color, and their intensity is usually described as non-luminescent, dully luminescent, and brightly luminescent. As a general rule, incorporation of Mn^{2+} into the calcite lattice stimulates luminescence and the incorporation of Fe^{2+} quenches or reduces

luminescence (Fairchild, 1983; Allan and Wiggins, 1993; Scholle and Ulmer-Scholle, 2003). Qualitative interpretation of CL usually assigns nonluminescent responses to oxidizing settings in which the reduced forms of both Mn and Fe are unavailable for incorporation into the lattices of carbonate mineral precipitates. Oxidized forms of Mn and Fe are not incorporated into calcite or dolomite crystals. Therefore, there is nothing in these crystals to excite luminescence. Bright luminescence is related to carbonate precipitates with high Mn/Fe trace element ratios, typically as a result of reducing environments during early (near-surface) to intermediate stages of burial diagenesis. Dull luminescence seems to happen where the Mn/Fe trace element ratios are present in carbonate precipitates. Thus, dull luminescence is usually thought to be the result of intermediate to late stages of burial diagenesis. It appears that elements other than Mn and Fe do not have any appreciable effect in enhancing or reducing luminescence (Budd and others, 2000).

Particularly useful references on the uses and limitations of CL interpretations in ancient carbonate studies include Sipple and Glover (1965), Frank and others (1982, 1996), Marshall (1988), Hemming and others (1989), Barker and Kopp (1991), Gregg and Karakus (1991), Machel (2000), Lavoie and others (2001), Coniglio and others (2003), and Lavoie and Morin (2004).

Previous Work

There is no known published work to date on the application of CL petrography on Pennsylvanian rocks from the Blanding sub-basin. Unpublished work includes observations of carbonate cements and dolomites in thin sections from Ismay zone outcrop samples along the San Juan River and from five Ismay zone cores in Ismay field by Brinton (1986).

Methodology

The analysis done in this study was completed using uncovered, polished thin sections, although rock chips and unpolished thin sections could be used. The equipment needed for CL can be installed on almost any polarizing microscope (see Marshall, 1988; Miller, 1988). A Nulcide Corporation luminocope model (figure 6; see also Marshall, 1988) belonging to the Colorado School of Mines Department of Geological Engineering was used for this analysis. Operating conditions were generally at 10-12kV accelerating potential, 0.5-0.7 mA of beam current and a beam focused at ~2 cm. All the work involved visual observations and some photographic documentation. Photomicrographs were taken using Fuji 1600 ASA color negative film. No attempt was made to measure intensities or spectral information on the CL responses (for example Marshall, 1991; Filippelli and Delaney, 1992) to the Ismay and Desert Creek samples. Image analysis and regional mapping of cement zones (that is "cement stratigraphy") have been done by some workers on carbonate cements (for example Meyers, 1974, 1978; Dorobek and others, 1987; Cander and others, 1988; Dansereau and Bourque, 2001), but these applications are beyond the scope of diagenesis documentation attempted in this project.

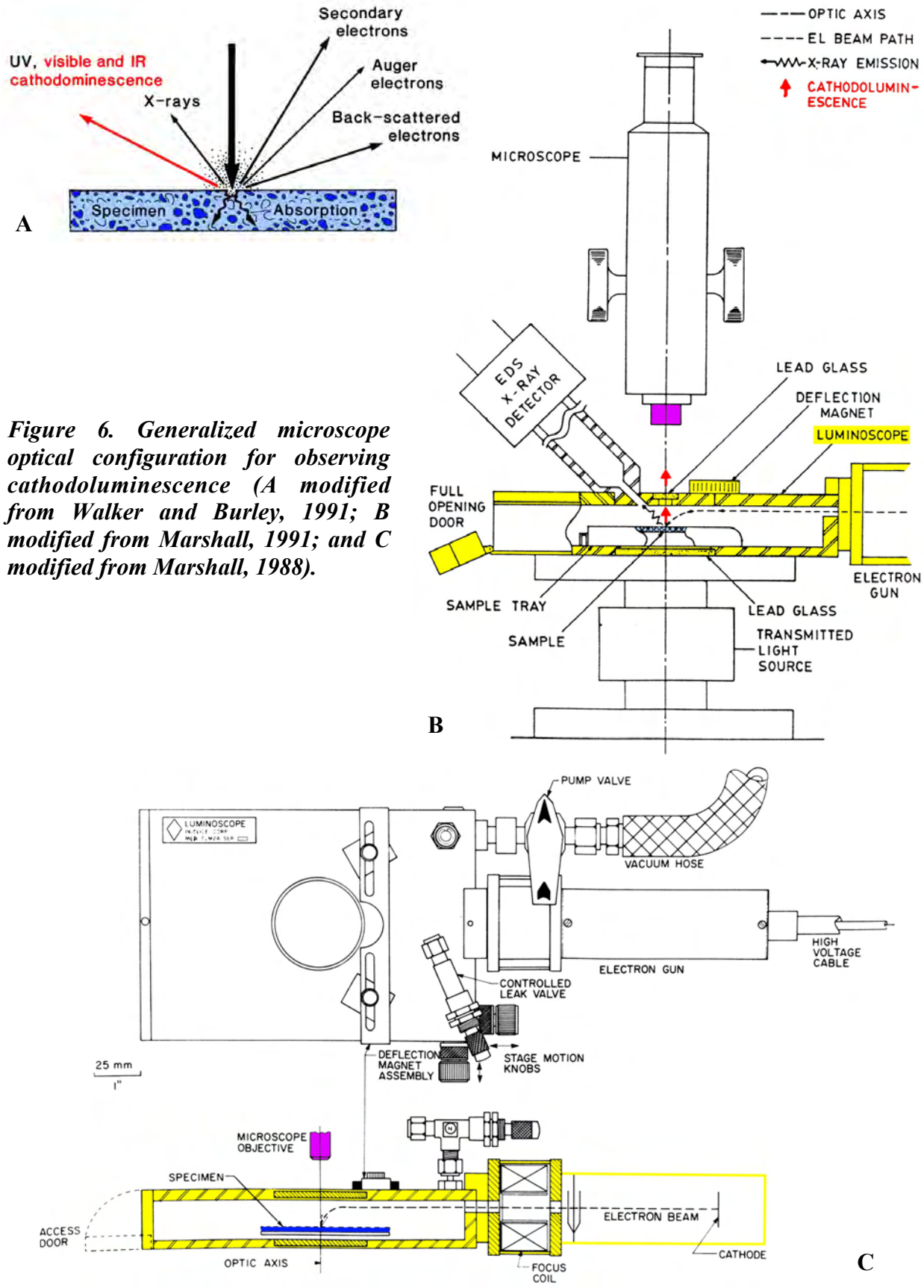

Figure 6. Generalized microscope optical configuration for observing cathodoluminescence (A modified from Walker and Burley, 1991; B modified from Marshall, 1991; and C modified from Marshall, 1988).

Cathodoluminescence Petrography of Upper Ismay and Lower Desert Creek Limestone and Dolomite Thin Sections

Cathodoluminescence examination was completed on five thin section samples from the upper Ismay zone limestones and dolomites within Cherokee field, and five samples of lower Desert Creek zone dolomite thin sections in Bug field (table 1; figures 2 and 4). In the Appendix of this report, there are 34 representative paired CL and transmitted plane light (Pl) photomicrographs from two of the Cherokee Federal No. 22-14 well upper Ismay samples, and five of the lower Desert Creek samples throughout Bug field. These thin section samples were selected to be representative of mineralogical (for example calcite, dolomite, anhydrite, and quartz), compositional, diagenetic, and pore types encountered within one core from the upper Ismay limestones of Cherokee field and within four cores from the lower Desert Creek dolomites of Bug field. In addition, short descriptive captions are included adjacent to each photomicrograph. A detailed description and interpretation of the CL and Pl petrography of each thin section sample illustrated in the Appendix follows.

Table 1. Upper Ismay (Cherokee field) and lower Desert Creek (Bug field) samples used for cathodoluminescence microscopy.

Well	Depth	Comments
Cherokee Fed. 22-14	5773.9	Tight dolomite with no visible fabrics or differences under CL. No photomicrograph examples in this report.
Cherokee Fed. 22-14	5778.1	Micro-porous dolomite; only dim to no visible CL differences. No photomicrograph examples in this report.
Cherokee Fed. 22-14	5821.2	Radiating cement crystals & microporosity. No photomicrograph examples in this report.
Cherokee Fed. 22-14	5836.8	Micro-zoned dolomite cements & bladed to equant calcite cements. Three pairs of photomicrographs included in report.
Cherokee Fed. 22-14	5870.3	Saddle dolomite replacement of limestone matrix & saddle dolomite cements. Three pairs of photomicrographs included in report.
May Bug 2	6306	Dolomitized micro-fibrous botryoidal cements. Two pairs of photomicrographs included in report.
May Bug 2	6312	Zone mega- and micro-dolomite crystals within brecciated fabric. Four pairs of photomicrographs included in report
Bug 10	6327.9	Alternating tight and streaks within dolomites. Three pairs of photomicrographs included in report.
Bug 13	5930.6	“Soil” pisolites and coated grain aggregates (grapestone?). Two pairs of photomicrographs included in report.
Bug 16	6300.5	Micro-box-work dolomite. One pair of photomicrographs included in this report.
TOTAL	**10 thin sections**	**18 CL-PL pairs of photomicrographs included in this report.**

Cathodoluminescence Petrography of Upper Ismay Thin Sections at Cherokee Field

Cathodoluminescence microscopy was completed on core sample thin sections with a variety of rock textures and diagenetic phases from the upper Ismay zone limestones within the Cherokee Federal No. 22-14 well (table 1). However, only two of the five samples showed any significant visible response to CL (see Appendix). The following remarks summarize our findings.

Cherokee Federal No. 22-14 well, 5836.8 feet: Cathodoluminescence imaging provides good to excellent resolution of grains (both skeletal and non-skeletal) as well as different generations of calcite cements within the limestone in this thin section. Fine details of the microstructures within skeletal fragments, such as brachiopods, bryozoans, and phylloid-algal plates, are more readily visible under CL than with transmitted plane light. In addition, calcite cements that rim leached skeletal grains, as well as early generations of isopachous cements, can be easily seen. Some of the cements display a series of concentric bright and dull luminescent bands that represent multiple generations of cementation under varying water chemistries. Such concentrically banded cements are similar to those cements used in calcite cement stratigraphy within Carboniferous carbonate systems in North America by Meyers (1974, 1978, 1991) and Goldstein (1988, 1991). Finally, CL makes it easier to see the pore outlines and boundaries than under plane light viewing. Thus, it becomes possible to qualitatively interpret how interconnected the remaining pore systems are within this sample.

Cherokee Federal No. 22-14 well, 5870.3 feet: Cathodoluminescence imaging was very useful in identifying the presence of saddle dolomites (Radke and Mathis, 1980) within microporous dolomites in this sample from the Cherokee Federal No. 22-14 well core. Large dolomite crystals (1.0 to 2.0 mm in diameter) with distinctly curved crystal faces occur as both replacements of finer, earlier dolomites and as pore-filling cements. These saddle dolomites display dull, red luminescence in their core areas and slightly bright, orange-red luminescence toward their rim areas. In addition, CL makes it possible to see the growth bands in these coarse dolomite crystals due to slight luminescent differences between each growth zone.

In general, the presence of saddle dolomites within a carbonate sample is indicative of the growth of strained, slightly iron-rich, dolomite replacements and cements under elevated temperatures during burial conditions (Radke and Mathis, 1980). Additional published descriptive work on saddle dolomites using CL may be found in Lavoie and Morin (2004).

Cathodoluminescence Petrography of Lower Desert Creek Thin Sections at Bug Field

Cathodoluminescence microscopy was completed on core sample thin sections exhibiting a variety of rock textures and diagenetic phases from the lower Desert Creek zone dolomites within the May Bug No. 2, Bug No. 10, Bug No. 13, and Bug No. 16 wells (table 1 and Appendix). The following remarks summarize our findings.

May Bug No. 2 well, 6306 feet: Cathodoluminescence imaging was used to examine the details of early, fibrous, marine cements that occur as distinct botryoidal fans within this Bug field sample of lower Desert Creek reservoir dolomites. Most of these fibrous cements exhibit fairly uniform orange and red luminescence. Hints or ghosts of the radiating cement fibers are visible. The blunt to squares ends of several radiating bundles of fibrous cements can be seen. These blunt ends have been used by some carbonate workers (Frank and others, 1982; Goldstein, 1988, 1991) to suggest original aragonite mineralogy of these cements, since modern aragonite botryoidal cements exhibit similar morphologies. In addition, small, internal dissolution pores crossing these early marine cements are also more readily visible using CL.

May Bug No. 2 well, 6312 feet: The dolomites replacing brecciated phylloid-algal mound fabrics are distinctly zoned when viewed under CL. Replacement dolomite crystals and crystal aggregates that average 100 to 200 μm display dull to non-luminescent cores and bright red luminescent rims. In one of the photomicrographs from this sample, up to four growth zones can be seen within individual dolomite rhombs. The resulting dolomitization and crystal size growth creates small sucrosic crystals that form an effective intercrystalline pore system. These intercrystalline pores augment the vuggy and shelter pores created by the brecciated phylloid-algal mound fabric. Cathodoluminescence imaging makes it easier to see the contacts between dolomite matrix and pores. Cathodoluminescence brings out significant detail in areas of anhydrite replacement of the dolomitized sediment. Islands of red luminescing dolomite can be easily seen within the plethora of bladed-anhydrite crystal aggregates. Within other portions of this sample, carbonate grains such as peloids and fragmented skeletal debris can be distinguished from carbonate cements in this completely dolomitized interval. The dolomitized grains exhibit deep red colors under CL while the carbonate cements are bright reddish orange. Finally, CL does an excellent job in imaging microfractures and microfracture swarms cutting through the lower Desert Creek dolomites. In this sample, an orthogonal set of microfractures cuts across the thin section. Most of these microfractures can be seen as the dark-gray to black (non-luminescent) curvilinear lines. It is possible that some of these open microfractures may have originated from dissolution along microstylolites.

Bug No. 10 well, 6327.5 feet: Cathodoluminescence imaging of this sample was particularly useful in identifying the shape and distribution of phylloid-algal plates, even though most of the plates have been partially dissolved, lined with early cements, and dolomitized. Micro-box-work arrays of bladed dolomite crystals are also very distinctive. In addition, CL provides a very vivid image of the distribution of both megapores and micropores within this dolomite. In particular, CL provides sharp definition of the pore boundaries with the dolomite matrix and crystal boundaries. Evidence of a brecciated fabric, as well as dissolution and corrosion of early sediments and cement, are easier to identify in this sample under CL than under plane polarized light.

Bug No. 13 well, 5930.6 feet: This sample consists of dolomitized pisolites and coated grain aggregates (similar to "grapestone"). Cathodoluminescence imaging aids in distinguishing the smaller grains incorporated into the grapestone, or aggregate grains, versus the early marine cements. Portions of this sample consist of internal sediment composed of carbonate mud and silt-sized, detrital quartz. The pelleted nature of the muddy portion of this sample is very evident under Cl, despite the complete dolomitization of this interval. Interestingly, detrital quartz silt grains of probable eolian origin are easily visible within the internal sediments of this sample. In addition, cathodoluminescence imaging makes it much easier to see the open (versus cemented) pores and microfractures within this sample.

Bug No. 16 well, 6300.5 feet: Cathodoluminescence imaging of this sample was particularly useful in identifying dense, dolomitized, micro-box-work arrays as well as bundles of fibrous marine cements. Original grains and cement fabrics can be seen in the brighter red portions of the luminescing dolomites. Somewhat later cements and zonation within coarser dolomites can be seen in the orangish-red areas. Cathodoluminescence imaging also provides sharp definition of rhombic dolomite crystal terminations as well as intercrystalline pores.

SUMMARY

1. Examination of upper Ismay limestones and lower Desert Creek dolomites under CL makes it possible to more clearly identify grain types and shapes, early cements (such as botryoidal, fibrous marine, bladed calcite cements), and brecciated phylloid-algal mound fabrics. In addition, identification of pelleted fabrics in muds, as well as various types of skeletal grains, is improved by CL examination in rocks where these grains have been poorly preserved, partially leached or completely dolomitized. In many ways, CL imaging of samples nicely complements the types of information derived from epifluorescence of carbonate thin sections.

2. Cathodoluminescence imaging clearly and rapidly images pore spaces that cannot be easily seen in standard viewing under transmitted, plane-polarized lighting. In addition, the cross sectional size, shape, and boundaries of pores are easy to determine. This information is often very useful when considering the origin and timing of dolomitization as well as evaluating the quality of the pore system within the dolomite.

3. Imaging of microfractures as well as dissolution along microstylolites, is greatly facilitated under CL. Many open microfractures cannot be easily seen in a normal 3-μm–thick petrographic thin section, especially within dense, lower Desert Creek dolomites. Routine CL examination of the same thin section often reveals the presence of individual microfractures or microfracture swarms.

4. Examination of saddle dolomites, when present within the clean carbonate intervals of the upper Ismay or lower Desert Creek interval, can provide more information about these late, elevated temperate (often hydrothermal) mineral phases. For instance, saddle dolomites from the Cherokee Federal No. 22-14 well showed nice growth banding. They also exhibited the difference between replacement and cement types of saddle dolomites under CL.

ACKNOWLEDGEMENTS

Core and petrophysical data were provided by Burlington Resources, Seeley Oil Company, and Wexpro Company. The Nuclide ELM 2-R Luminoscope used for this study is part of the instrumentation in the Department of Geological Engineering, Colorado School of Mines. John Humphrey assisted with the setup and instruction on this instrument.

James Parker and Cheryl Gustin of the Utah Geological Survey (UGS) drafted the figures. The report was reviewed by David Tabet and Michael Hylland of the UGS. Cheryl Gustin, UGS, formatted the manuscript for publication.

REFERENCES

Allan, J.R., and Wiggins, W.D., 1993, Dolomite reservoirs - geochemical techniques for evaluating origin and distribution: American Association of Petroleum Geologists, Continuing Education Course Note Series 36, 129 p.

Barker, C.E., and Kopp, O.C., editors, 1991, Luminescence microscopy - quantitative and qualitative aspects: Society for Sedimentary Geology (SEPM) Short Course 25 Notes, p. 1-7.

Brinton, L., 1986, Deposition and diagenesis of Middle Pennsylvanian (Desmoinesian) phylloid algal banks, Paradox Formation, Ismay zone, Ismay field and San Juan Canyon, Paradox Basin, Utah and Colorado: Golden, Colorado School of Mines, M.S. thesis, 315 p.

Budd, D.A., Hammes, U., and Ward, W.B., 2000, Cathodoluminescence in calcite cements - new insights on Pb and Zn sensitizing, Mn activation, and Fe quenching at low trace-element concentrations: Journal of Sedimentary Petrology, v. 70, p. 217-226.

Cander, H.S., Kauffman, J., Daniels, L.D., and Meyers, W.J., 1988, Regional dolomitization in the Burlington-Keokuk Formation (Mississippian), Illinois and Missouri - constraints from cathodoluminescent zonal stratigraphy, *in* Shukla, V., and Baker, P.A., editors, Sedimentology and geochemistry of dolostones: Society for Sedimentary Geology (SEPM) Special Publication No. 43, p. 129-144.

Coniglio, M., Zheng, Q., and Carter, T.R., 2003, Dolomitization and recrystallization of Middle Silurian reefs and platformal carbonates of the Guelph Formation, Michigan Basin, southwestern Ontario: Bulletin of Canadian Petroleum Geology, v. 51, p. 177-199.

Crawley-Stewart, C.L., and Riley, K.F., 1993, Cherokee, *in* Hill, B.G., and Bereskin, S.R., editors, Oil and gas fields of Utah: Utah Geological Association Publication 22, non-paginated.

Dansereau, P., and Bourque, P.A., 2001, The Neigette breccia - remnant of the West Point reef tract in the Matapedia Valley area, and witness to Late Silurian synsedimentary faulting, Gaspe Belt, Northern Appalachians, Quebec: Bulletin of Canadian Petroleum Geology, v. 49, p. 327-345.

Dorobek, S.L., Read, J.F., Niemann, J.M., Pong, T.C., and Haralick, R.M., 1987, Image analysis of cathodoluminescence-zoned calcite cements: Journal of Sedimentary Petrology, v. 57, p. 766-770.

Fairchild, I.J., 1983, Chemical studies of cathodoluminescence of natural dolomites and calcites: Sedimentology, v. 30, p. 572-583.

Filippelli, G.M., and DeLaney, M.L., 1992, Quantifying cathodoluminescent intensity with an on-line camera and exposure meter: Journal of Sedimentary Petrology, v. 62, p. 724-725.

Frank, J.R., Carpenter, A.B., and Oglesby, T.W., 1982, Cathodoluminescence and composition of calcite cement in Taum Sauk Limestone (Upper Cambrian), southeast Missouri: Journal of Sedimentary Petrology, v. 52, p. 631-638.

Frank, T.D., Lohmann, K.C., and Meyers, W.J., 1996, Chemostratigraphic significance of cathodoluminescence zoning in syntaxial cement - Mississippian Lake Valley Formation, New Mexico: Sedimentary Geology, v. 105, p. 29-50.

Goldstein, R.H., 1988, Cement stratigraphy of Pennsylvanian Holder Formation, Sacramento Mountains, New Mexico: American Association of Petroleum Geologists Bulletin, v. 72, p. 425-438.

---1991, Practical aspects of cement stratigraphy with illustrations from Pennsylvanian limestone and sandstone, New Mexico and Kansas, *in* Barker, C.E., and Kopp, O.C., editors, Luminescence microscopy - quantitative and qualitative aspects: Society for Sedimentary Geology (SEPM) Short Course 25 Notes, p. 123-131.

Gregg, J.M., and Karakus, M., 1991, A technique for successive cathodoluminescence and reflected light microscopy: Journal of Sedimentary Petrology, v. 61, p. 613-635.

Harr, C.L., 1996, Paradox oil and gas potential of the Ute Mountain Ute Indian Reservation, *in* Huffman, A.C., Jr., Lund, W.R., and Godwin, L.H., editors, Geology of the Paradox Basin: Utah Geological Association Publication 25, p. 13-28.

Harry, D.L., and Mickus, K.L., 1998, Gravity constraints on lithospheric flexure and the structure of the late Paleozoic Ouachita orogen in Arkansas and Oklahoma, south-central North America: Tectonics, v. 17, no. 2, p. 187-202.

Hemming, N.G., Meyers, W.J., and Grams, J.C., 1989, Cathodoluminescence in diagenetic calcites - the roles of Fe and Mn as deduced from electron probe and spectrophotometric measurements: Journal of Sedimentary Petrology, v. 59, p. 404-411.

Hintze, L.F., 1993, Geologic history of Utah: Brigham Young University Geology Studies Special Publication 7, 202 p.

Hite, R.J., Anders, D.E., and Ging, T.G., 1984, Organic-rich source rocks of Pennsylvanian age in the Paradox Basin of Utah and Colorado, *in* Woodward, Jane, Meissner, F.F., and Clayton, J.L., editors, Hydrocarbon source rocks of the greater Rocky Mountain region: Rocky Mountain Association of Geologists Guidebook, p. 255-274.

Kluth, C.F., 1986, Plate tectonics of the Ancestral Rocky Mountains: American Association of Petroleum Geologists Memoir 41, p. 353-369.

Kluth, C.F., and Coney, P.J., 1981, Plate tectonics of the Ancestral Rocky Mountains: Geology, v. 9, p. 10-15.

LaVoie, D., Chi G., and Fowler, M.G., 2001, The Lower Devonian Upper Gaspe Limestones in eastern Gaspe - carbonate diagenesis and reservoir potential: Bulletin of Canadian Petroleum Geology, v. 49, p. 346-365.

LaVoie, D., and Morin, C., 2004, Hydrothermal dolomitization in the Lower Silurian Sayabee Formation in northern Gaspe – Matapedia (Quebec) - constraint on timing of porosity and regional significance for hydrothermal reservoirs: Bulletin of Canadian Petroleum Geology, v. 52, p. 256-269.

Machel, H.G., 2000, Application of cathodoluminescence to carbonate diagenesis, *in* Pagel, M., Barbin, V., Blanc P., and Ohnenstetter, D., editors, Cathodoluminescence in geosciences: New York, Springer, p. 271-301.

Machel, H.G., and Burton, E.A., 1991, Factors governing cathodoluminescence in calcite and dolomites and their implications for studies of carbonate diagenesis, *in* Barker, C.E., and Kopp, O.C., editors, Luminescence microscopy - quantitative and qualitative aspects: Society for Sedimentary Geology (SEPM) Short Course 25 Notes, p. 37-57.

Marshall, D.J., 1988, Cathodoluminescence of geological materials: Winchester, Massachusetts, Allen & Unwin, 128 p.

---1991, Combined cathodoluminescence and energy dispersive spectroscopy, *in* Barker, C.E., and Kopp, O.C., editors, Luminescence microscopy - quantitative and qualitative aspects: Society for Sedimentary Geology (SEPM) Short Course 25 Notes, p. 27-36.

Martin, G.W., 1983, Bug, *in* Fassett, J.E., editor, Oil and gas fields of the Four Corners area, volume III: Four Corners Geological Society, p. 1073-1077.

Meyers, W.J., 1974, Carbonate cement stratigraphy of the Lake Valley Formation (Mississippian), Sacramento Mountains, New Mexico: Journal of Sedimentary Petrology, v. 44, p. 837-861.

---1978, Carbonate cements: their regional distribution and interpretation in Mississippian limestones of southwestern New Mexico: Sedimentology, v. 25, p. 371-400.

---1991, Cement stratigraphy - an overview, *in* Barker, C.E., and Kopp, O.C., editors, Luminescence microscopy - quantitative and qualitative aspects: Society for Sedimentary Geology (SEPM) Short Course 25 Notes, p. 133-148.

Miller, J., 1988, Cathodoluminescence microscopy, *in* Tucker, M., editor, Techniques in sedimentology: Oxford, Blackwell Publications, p. 174-190.

Nuccio, V.F., and Condon, S.M., 1996, Burial and thermal history of the Paradox Basin, Utah and Colorado, and petroleum potential of the Middle Pennsylvanian Paradox Formation, *in* Huffman, A.C., Jr., Lund, W.R., and Godwin, L.H., editors, Geology of the Paradox Basin: Utah Geological Association Publication 25, p. 57-76.

Oline, W.F., 1996, Bug, *in* Hill, B.G., and Bereskin, S.R., editors, Oil and gas fields of Utah: Utah Geological Association Publication 22 Addendum, non-paginated.

Radke, B.M., and Mathis, R.L., 1980, On the formation and occurrence of saddle dolomite: Journal of Sedimentary Petrology, v. 50, p. 1149-1168.

Scholle, P.A., and Ulmer-Scholle, D.S., 2003, A color guide to the petrography of carbonate rocks: American Association of Petroleum Geologists Memoir 77, 474 p.

Sipple, R.F., and Glover, E.D., 1965, Structures in carbonate rocks made visible by luminescence petrography: Science, v. 150, p. 1283-1287.

Utah Division of Oil, Gas and Mining, 2004, Oil and gas production report, November: non-paginated.

Walker, G., and Burley, S., 1991, Luminescence petrography and spectroscopic studies of diagenetic minerals, *in* Barker, C.E., and Kopp, O.C., editors, Luminescence microscopy - quantitative and qualitative aspects: Society for Sedimentary Geology (SEPM) Short Course 25 Notes, p. 83-96.

APPENDIX

THIN SECTION CATHODOLUMINESCENCE AND DESCRIPTIONS, CHEROKEE AND BUG FIELDS, SAN JUAN COUNTY, UTAH

CHEROKEE FEDERAL NO. 22-14 WELL, CHEROKEE FIELD

5836.8 feet

Top Photomicrograph

Cathodoluminescence overview of a representative skeletal/peloidal grainstone shows the details of grain preservation as well as different generations of calcite cement. Note the elongate non-luminescent area (from the upper left to right-central portions of this micrograph) which represents a dissolved phylloid-algal plate which is now a moldic pore. Other non-luminescent (black) portions of this view are also open pores or are filled with the same generation of calcite cement. A series of banded bright and dull cement generations represent an earlier generation of pore-filling cements.

Bottom Photomicrograph

The same field of view is shown here under Pl at the same magnification. Note that the preservation of original grains, leached skeletal grains such as the dissolved phylloid-algal plate, and the multiple generations of cement are not visible under plane light. Without CL, many of these features would be difficult to identify.

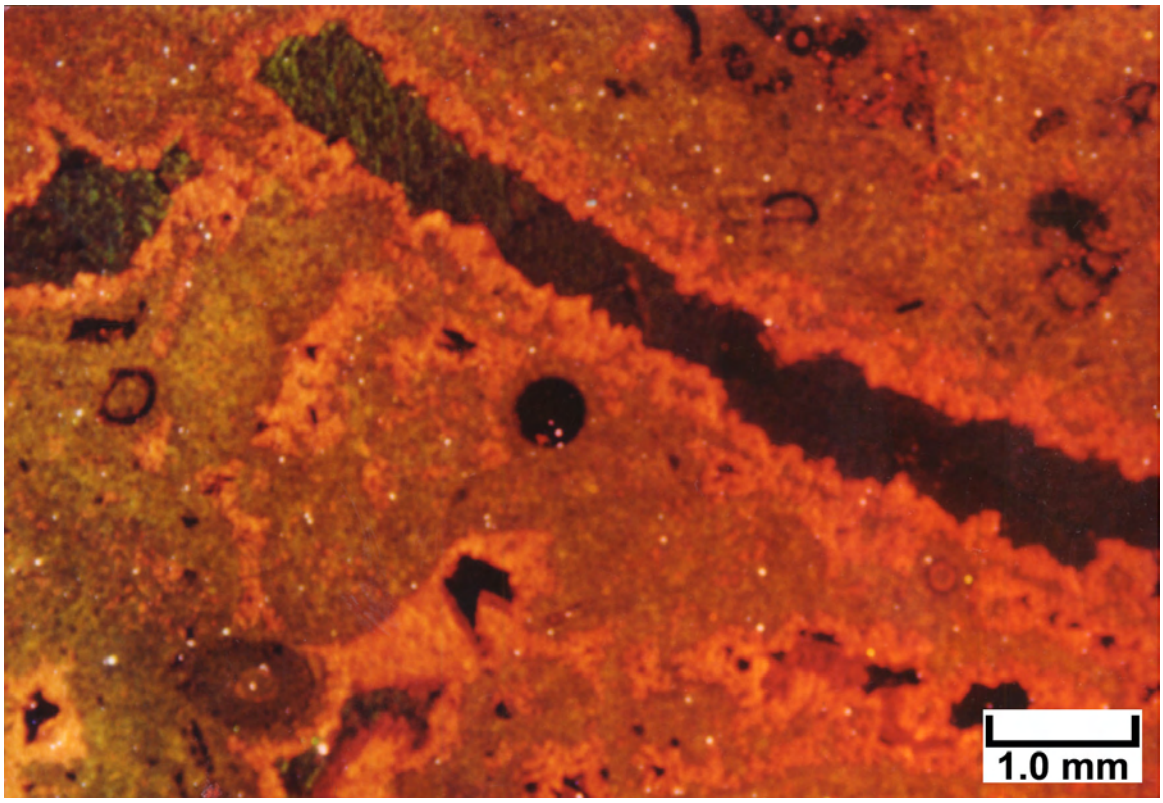
1.0 mm

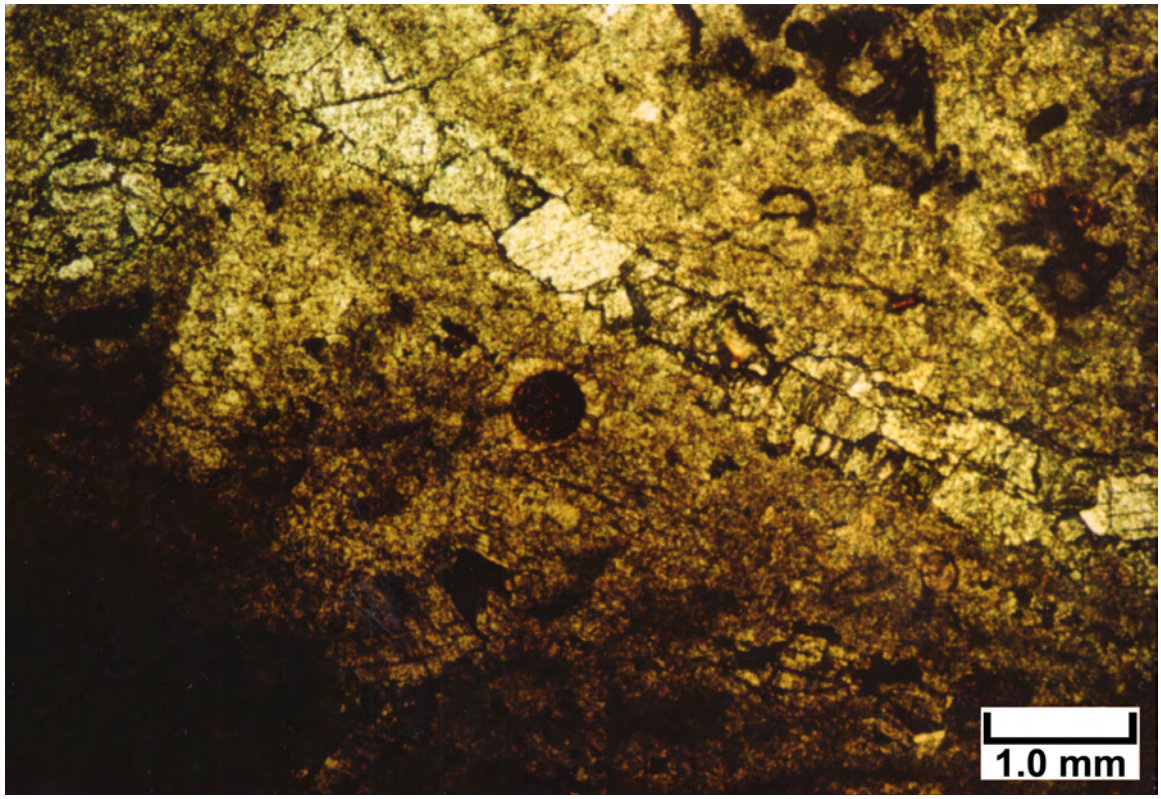
1.0 mm

5836.8 feet

Top Photomicrograph

This CL view shows various skeletal grains in the dull red shapes and colors surrounded by banded generations of early pore-filling cements. Note the non-luminescent (black) patches that represent largely secondary pores that have either been filled with equant calcite spar cement, or are isolated, open moldic pores. The numerous light blue specs across this micrograph are mostly detrital quartz silt grains within this carbonate sediment.

Bottom Photomicrograph

The same field of view is shown here under Pl at the same magnification. Vague outlines of skeletal grains, including broken phylloid-algal plates, brachiopod shells, and bryozoan fragments, are seen in the dark grains. This view does not provide much detail to differentiate various generations of calcite cement seen in CL view above.

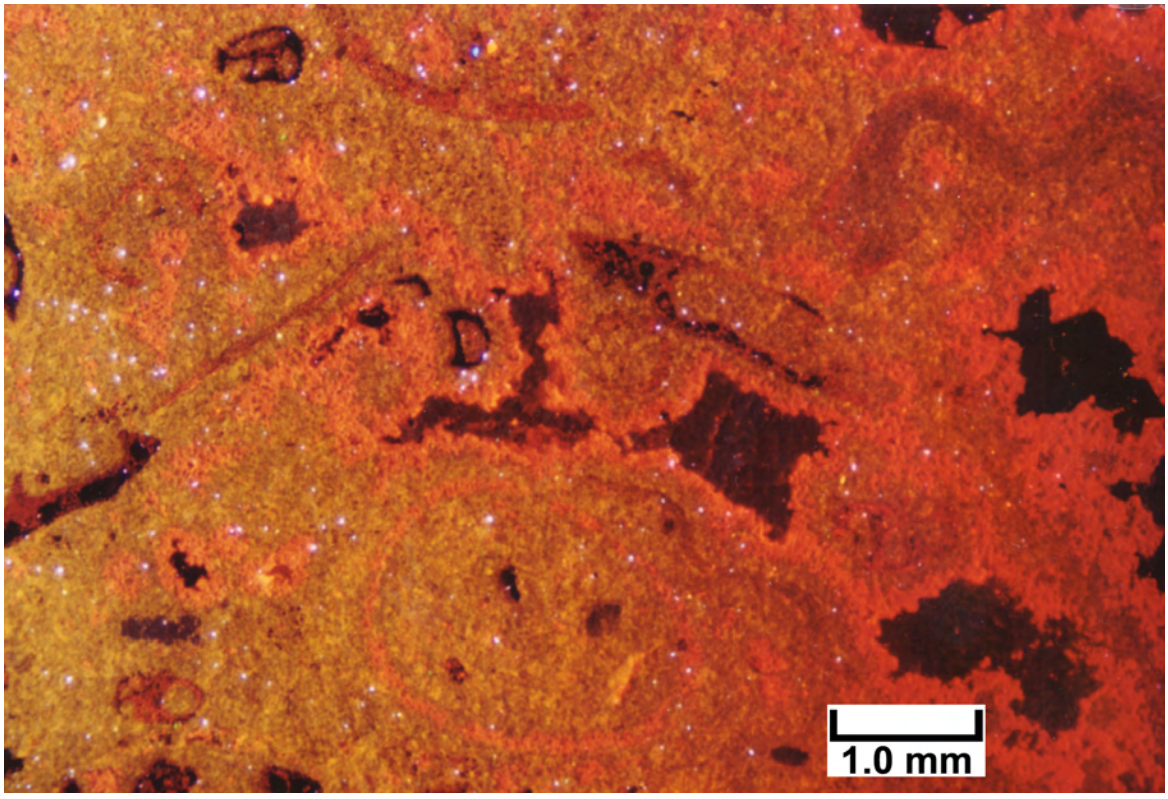
1.0 mm

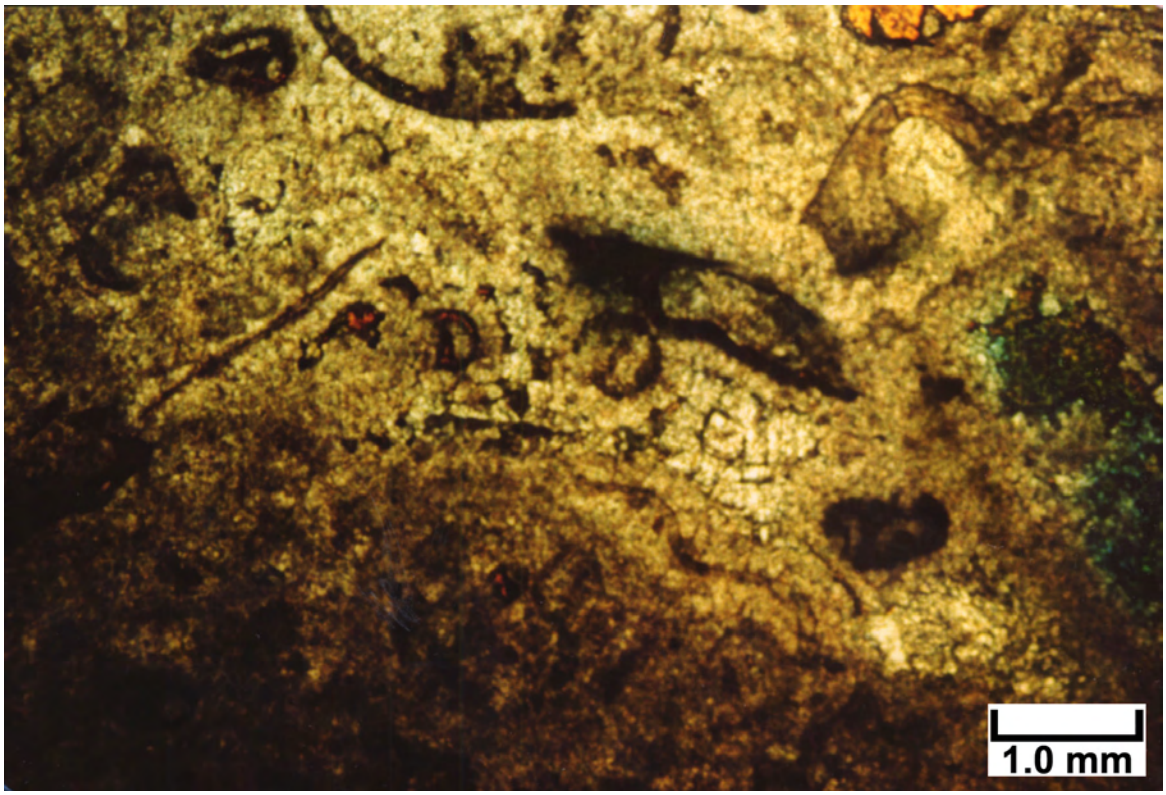
1.0 mm

5836.8 feet

Top Photomicrograph

Generations of isopachous cements surrounding skeletal grains are shown here as banded luminescent cements. As in the previous CL micrographs from this depth, the black (non-luminescent) patches consist of late calcite spar filling largely secondary pores, or are open pores. The burnt orange patches across the top of this micrograph consist of late replacement of this limestone by bladed anhydrite.

Bottom Photomicrograph

The same field of view is shown here under Pl at the same magnification. Note that it is virtually impossible to distinguish skeletal grains from cement generations. In addition, details of the late anhydrite replacement are not clear under Pl.

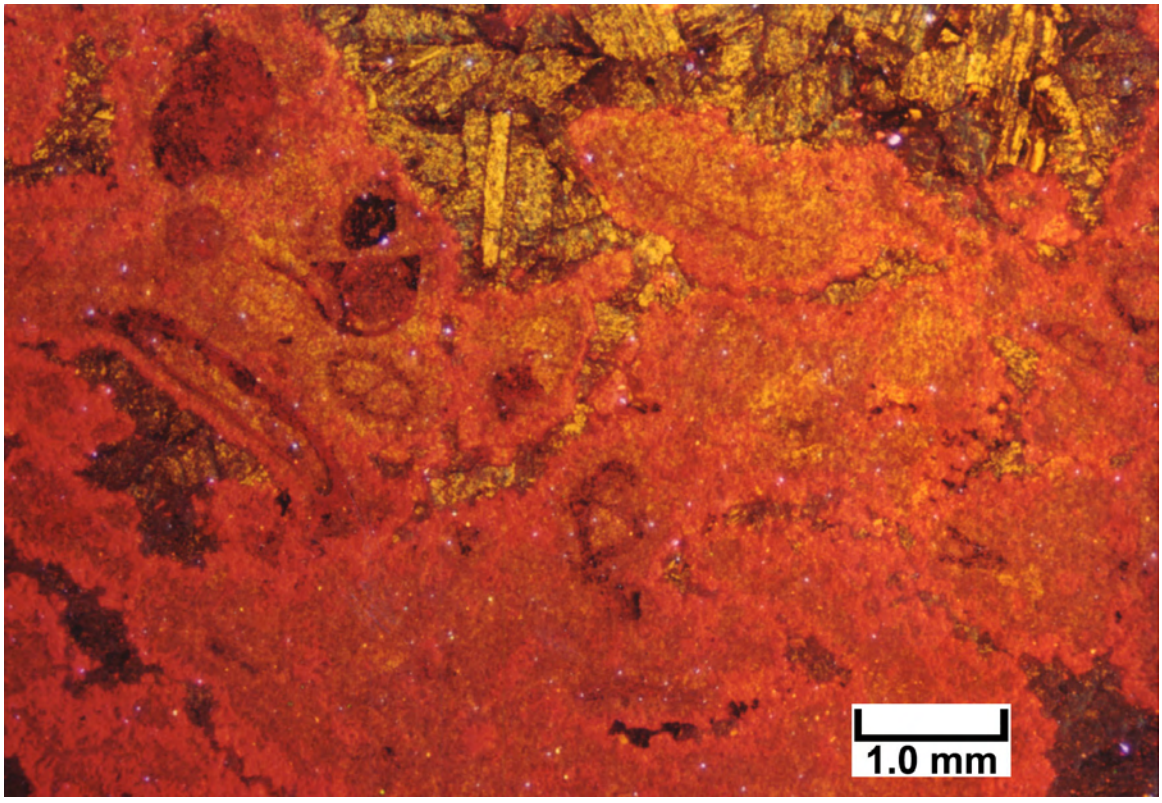
1.0 mm

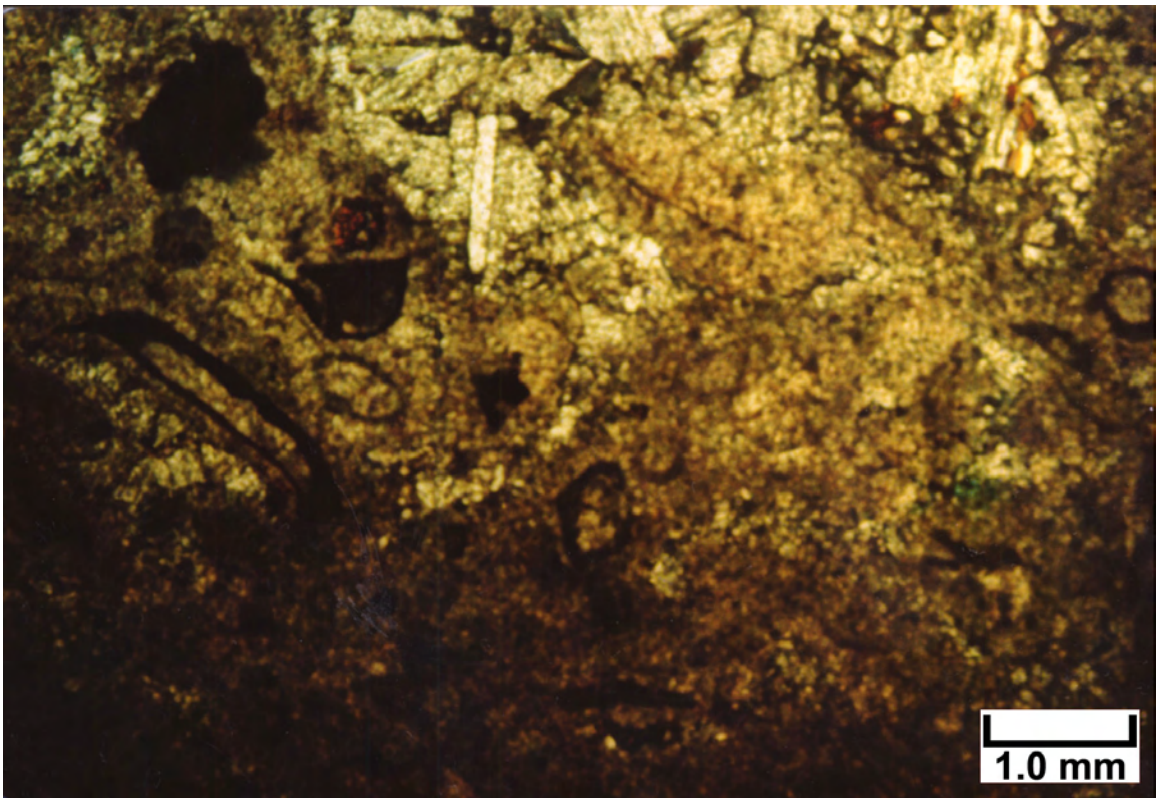
1.0 mm

5870 feet

Top Photomicrograph

Most of the large crystals in this CL view consist of dolomite. Note in particular that the large crystal in the center displays strongly curved crystal faces. This "saddle dolomite" (see Radke and Mathis, 1980) as well as the other coarse dolomite crystals with reddish luminescence are probably late, burial or hydrothermal dolomites that precipitated under elevated temperatures.

Bottom Photomicrograph

The same field of view is shown here under cross-polarized light at the same magnification. Note the sweeping extinction within the large crystal in the center, indicative of a strained crystal lattice. The bluish areas surrounding these replacement dolomites are remnants of intercrystalline pores.

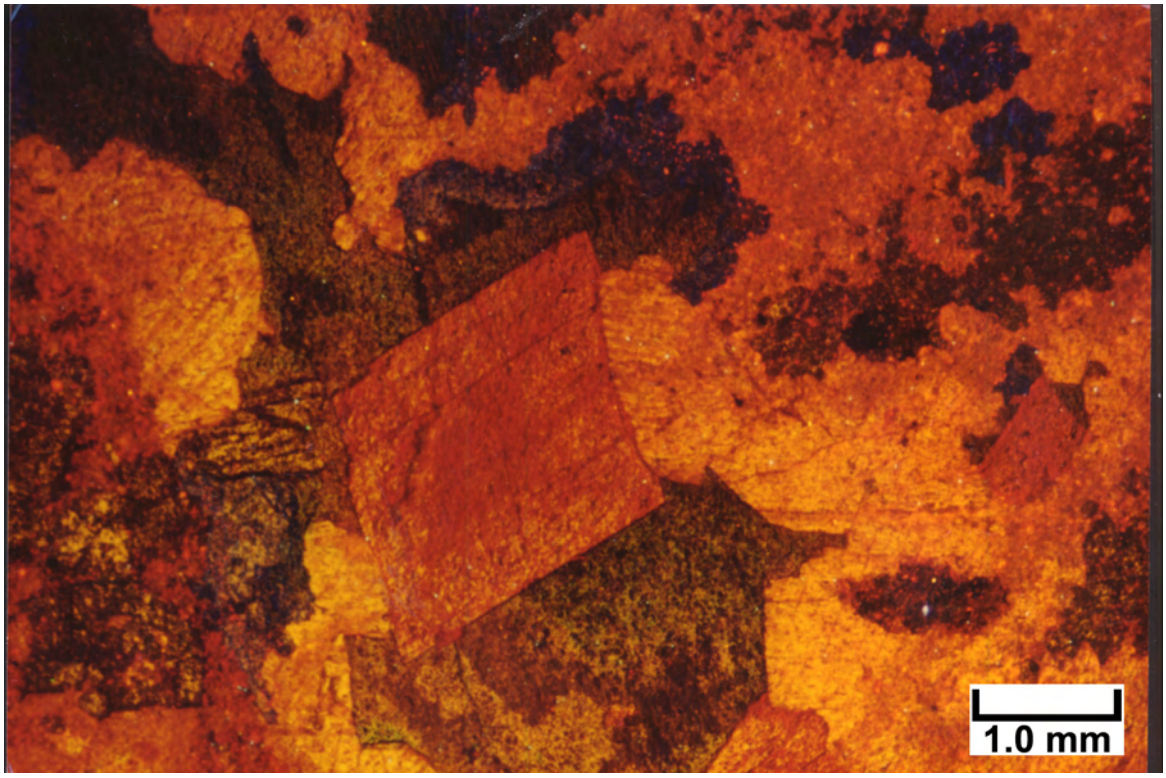
1.0 mm

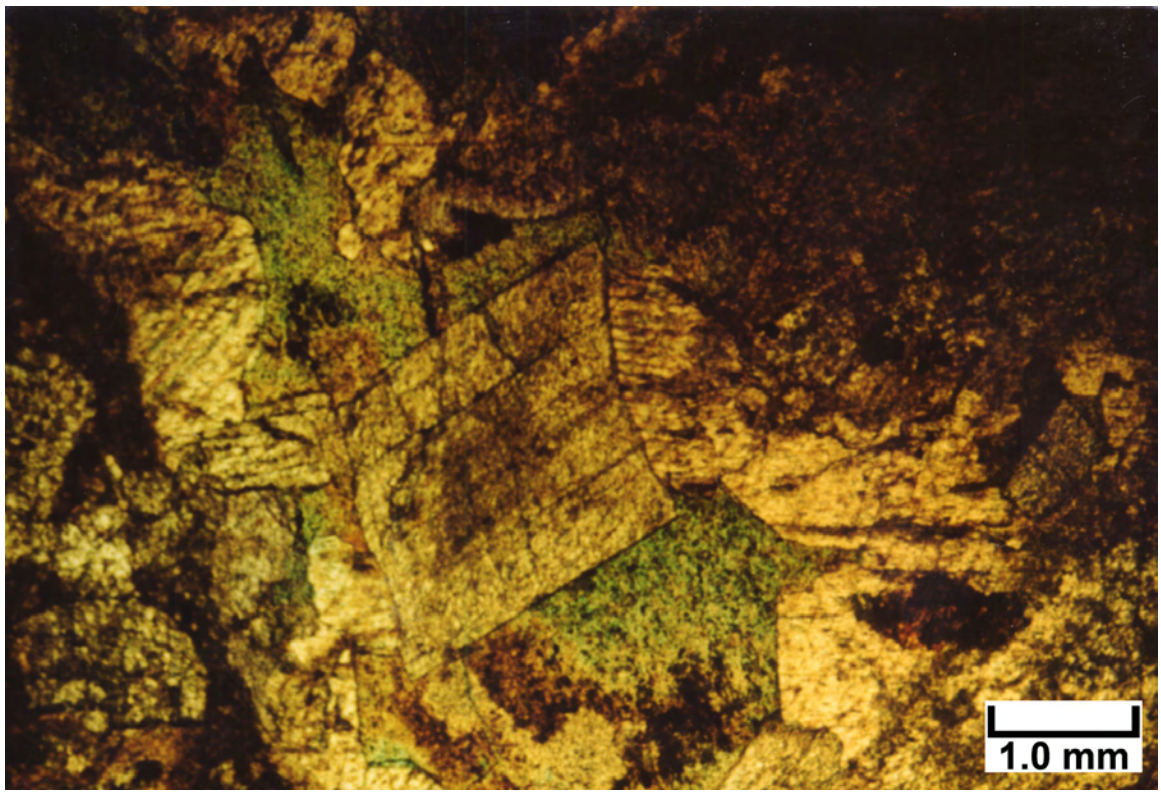
1.0 mm

5870 feet

Top Photomicrograph

This CL view shows remnants of a muddy limestone matrix (wackestone) in the lower left and upper right corners of this micrograph that has been partially replaced by coarse dolomite crystals displaying curved faces. These "saddle dolomites" have a distinctive dull red and orange luminescence in which hints of the dolomite growth bands can be seen. Small inclusions of dark-colored, lime, wackestone matrix can be seen scattered throughout the coarse dolomite saddles, indicating that these saddle dolomites are replacing previous carbonates rather than being entirely cements.

Bottom Photomicrograph

The same field of view is shown here under cross-polarized light at the same magnification. Note the intercrystalline pores (blue areas) between some of the saddle dolomites. This view makes it possible to see where dolomite has replaced lime wackestone matrix (in the medium and dark brown areas) and where dolomite is a cement growing into open pores (the clear areas).

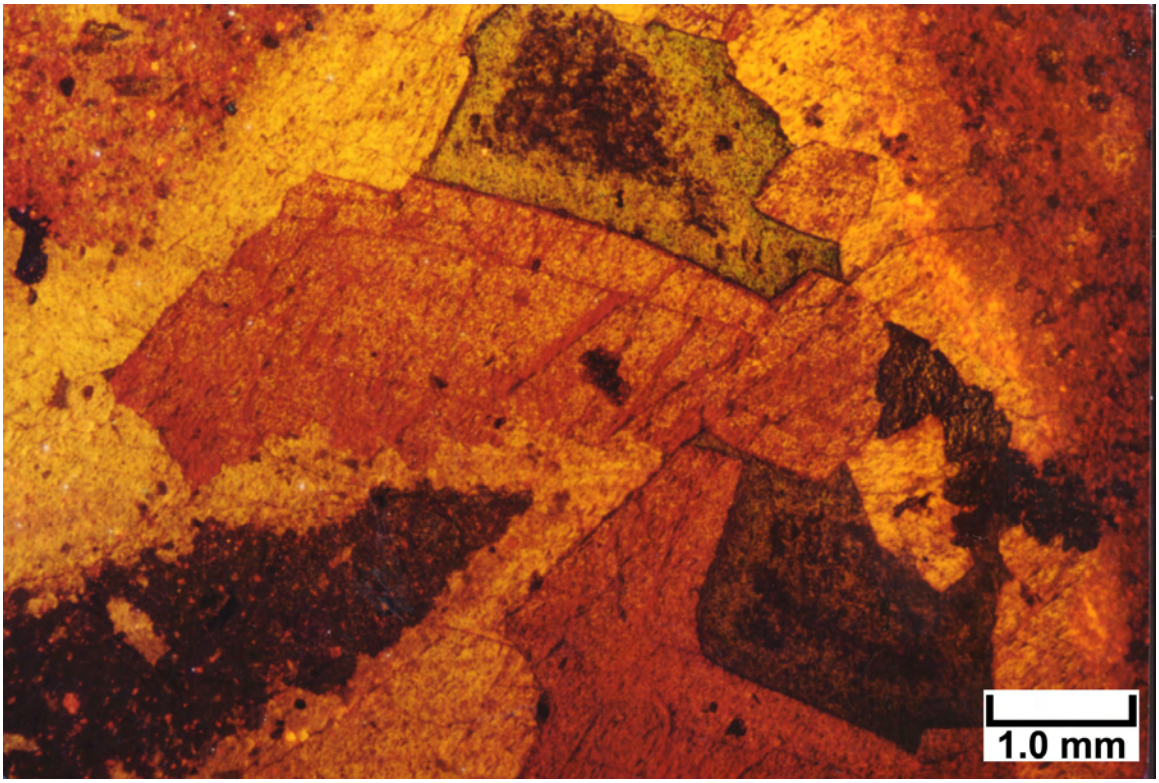
1.0 mm

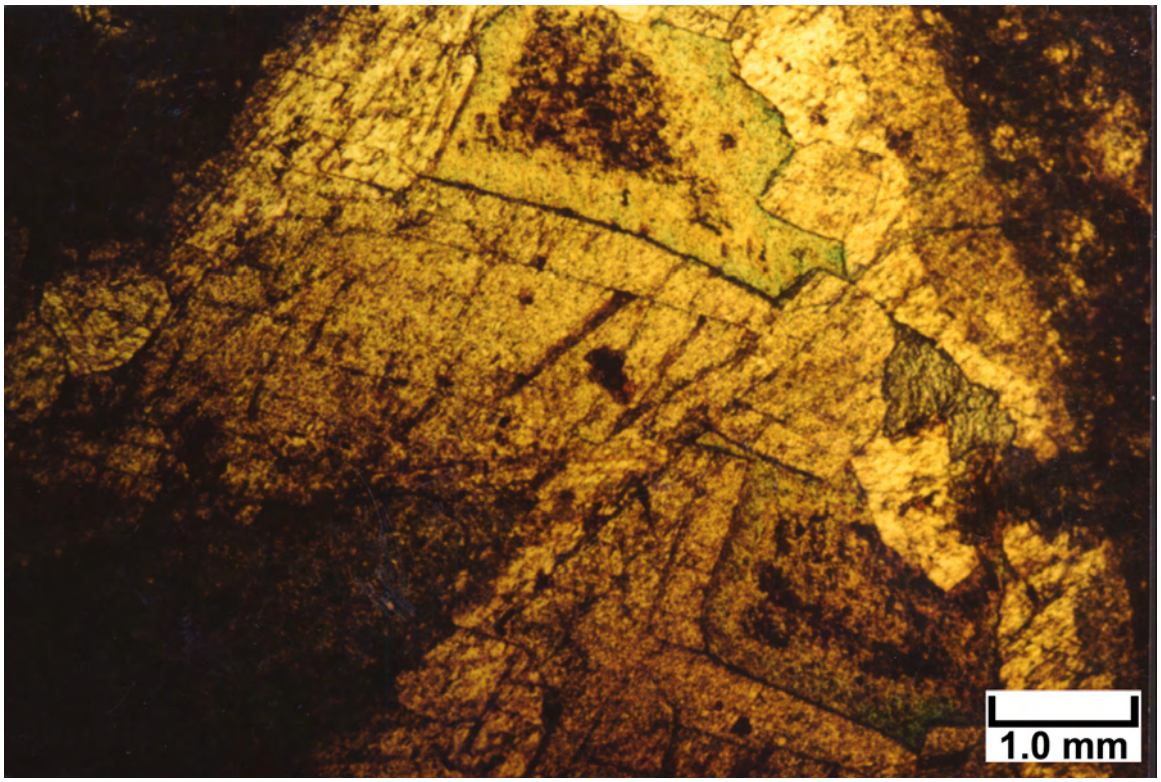
1.0 mm

MAY BUG NO. 2 WELL,
BUG FIELD

6306 feet

Top Photomicrograph

Cathodoluminescence imaging of a large botryoidal fan of dolomitized cements (originally aragonite) shows reasonably uniform orange and red luminescence. Note the blunt-shaped or square-ended crystal bundles evident in the area just to the right of center. Hints of radiating fibrous cements can be seen from bottom of the photograph to the top in this view. The black (non-luminescent) patches represent secondary pores within these early marine botryoidal cements.

Bottom Photomicrograph

The same field of view is shown here under Pl at the same magnification. This micrograph shows ghosts of the radiating fibrous crystal habit of these completely dolomitized, early marine botryoidal cements. Without the CL view (see above), it would be difficult to see either the blunt crystal fan terminations or the dissolution pores.

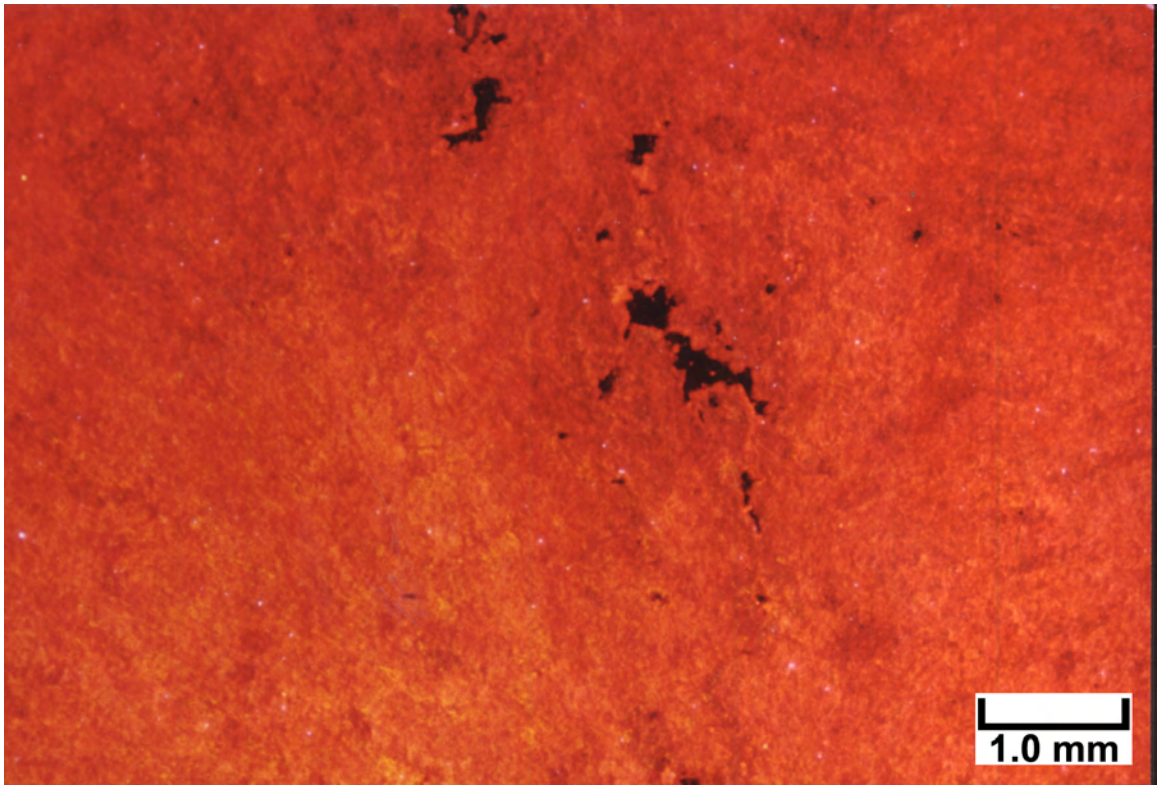
1.0 mm

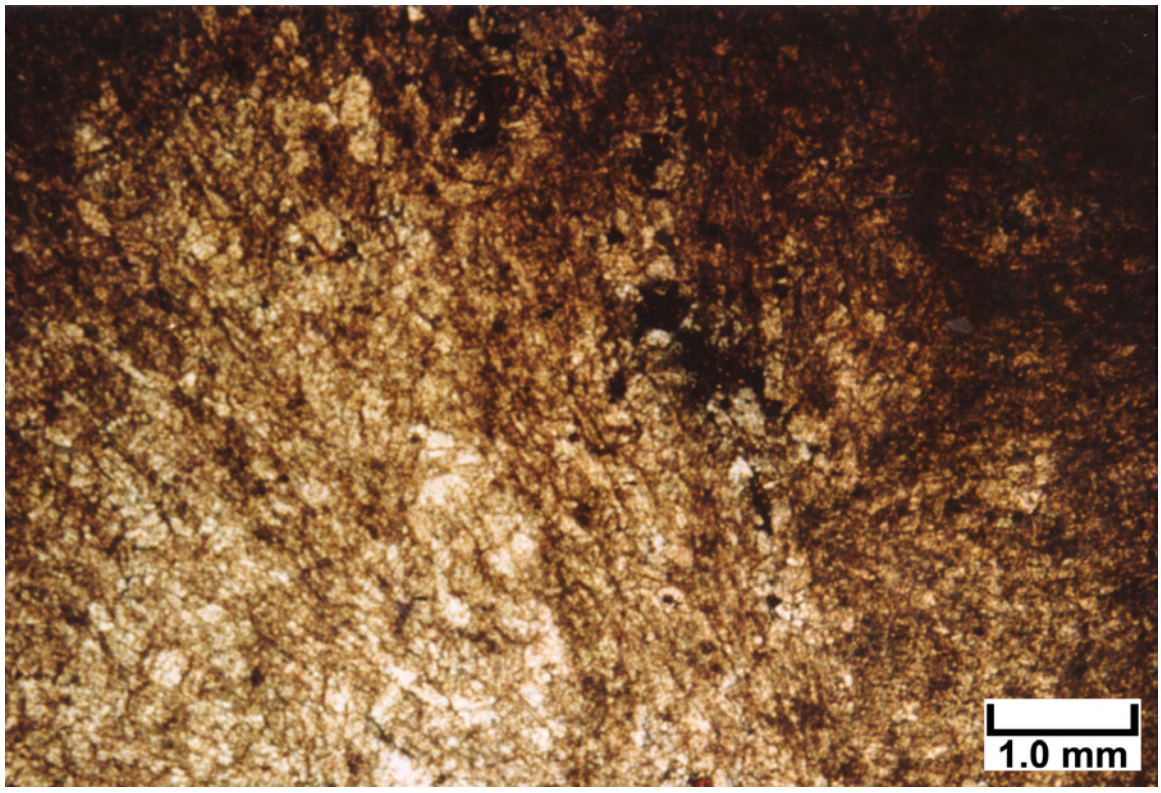
1.0 mm

6306 feet

Top Photomicrograph

This CL view cuts across fibrous calcite (originally aragonite) crystal fans that are part of botryoidal cement precipitated between brecciated phylloid-algal mounds. Despite the fairly uniform dull luminescence of these cements, it is possible to see hints of the radiating fibrous crystal bundles (in general, radiating from left to right). The black (non-luminescent) patches were originally dissolution pores within these botryoidal cements.

Bottom Photomicrograph

The same field of view is shown here under Pl at the same magnification. Except for ghosts of fibrous crystal bundles at various orientations, it is difficult to see much detail within these botryoidal cements without viewing under CL. Note that the root beer-colored crystals in this view are calcite spars and pore-filling epoxy that have been discolored by the electron beam during viewing under CL.

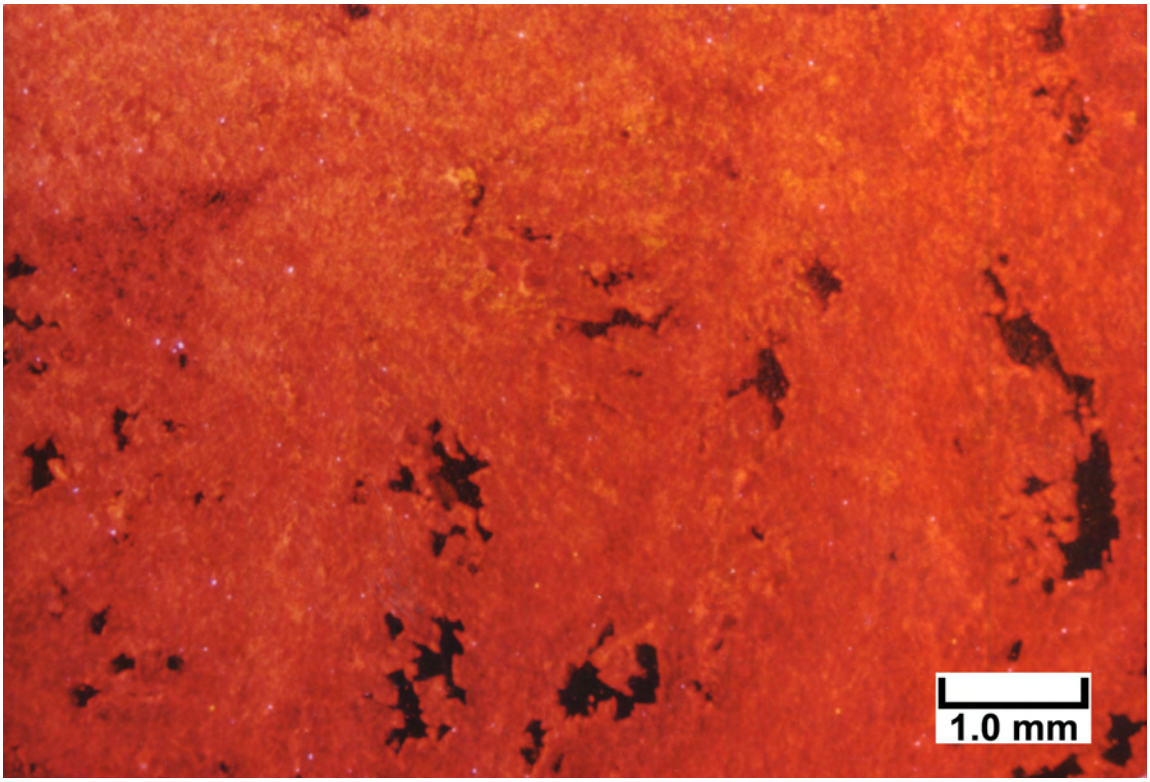
1.0 mm

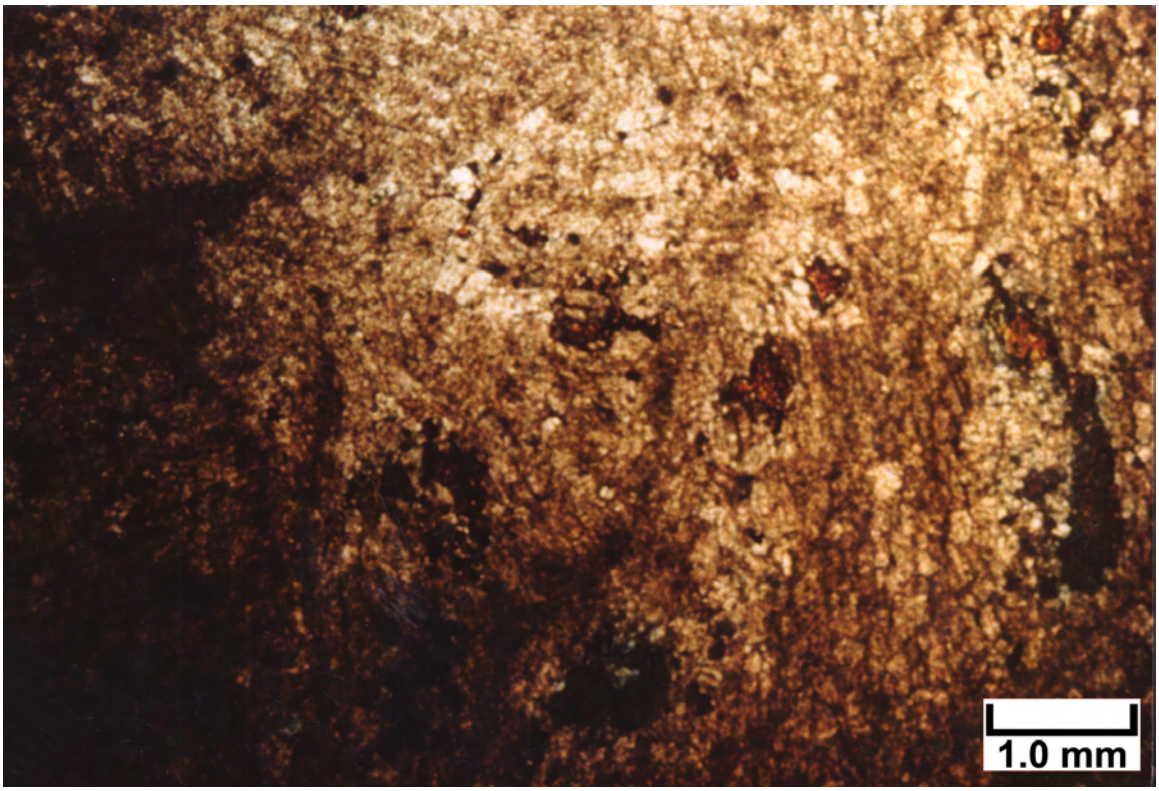
1.0 mm

6312 feet

Top Photomicrograph

This CL view nicely shows micro-rhombic dolomites that have completely replaced a brecciated phylloid-algal mound fabric. Despite the dull red luminescence of these dolomites, growth zones and different crystal sizes can readily be seen within the replacement fabric. For instance, note the dolomite crystals (in the upper center portion of this micrograph) with dead (black) cores and bright luminescent (red) rims. This zonation is probably related to two distinct growth stages of this replacement dolomite. The resulting dolomitization of this mound fabric creates small sucrosic or rhombic crystals that produce an effective intercrystalline pore system. The large black patches in the lower half of this micrograph consist of open pores within this brecciated phylloid-algal mound fabric.

Bottom Photomicrograph

The same field of view is shown here under Pl at the same magnification. Note that there is very little detail within this replacement dolomite that is visible under plane-transmitted light. For instance, it is impossible to see any of the zoned dolomite rhombs or the precursor fabrics before dolomite replacement without the use of CL.

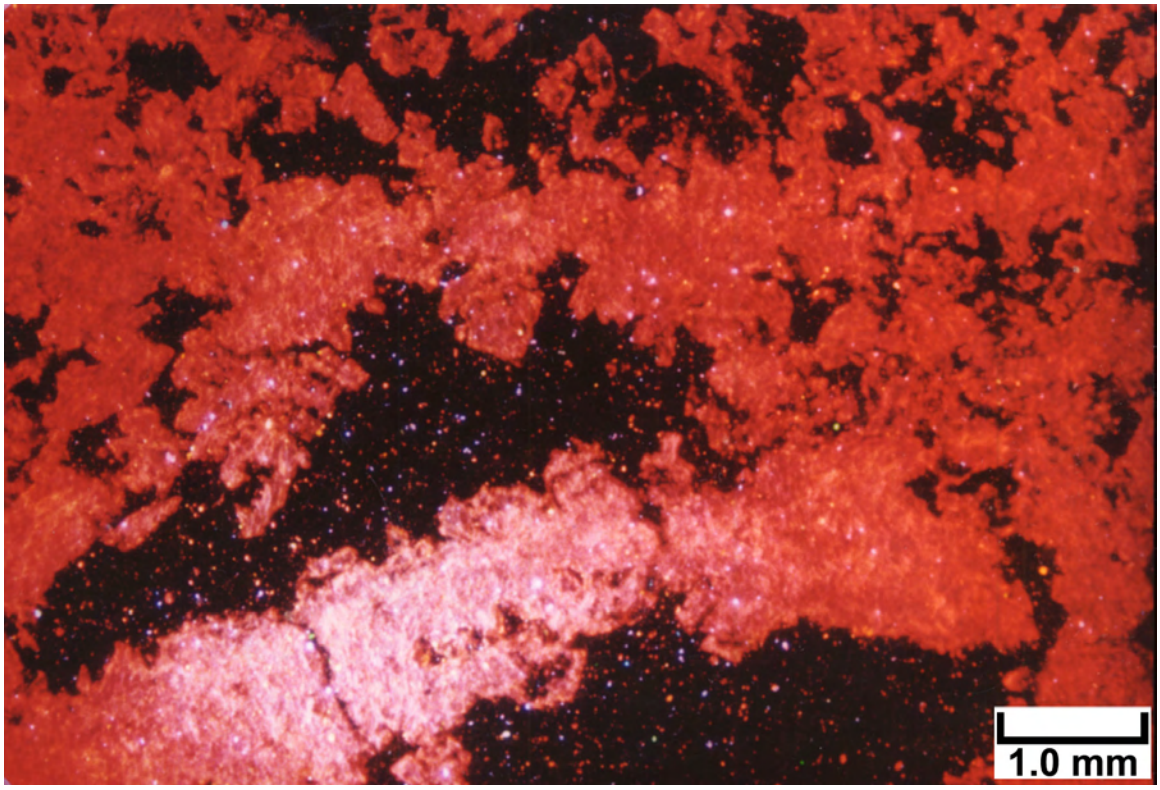
1.0 mm


1.0 mm

6312 feet

Top Photomicrograph

Cathodoluminescence imaging of this completely dolomitized phylloid-algal mound fabric shows a number of interesting features. Note the ghost of a large phylloid-algal plate (from bottom center to right center) which was partially dissolved out and is now filled with micro-zoned dolomite crystals. These zoned crystals can be observed by the alternating dull and bright red bands within the dolomite rhombs. Some rhombs appear to have as many as four growth zones. The left half of this micrograph shows carbonate skeletal grains and internal sediments that have been replaced by micro-rhombic dolomites. The large black patch in the upper left consists mostly of an open dissolution pore. Finally, the dull brownish luminescence along the right hand margin of this micrograph nicely shows bladed replacement anhydrite following dolomitization of this carbonate sediment. Islands of original dolomite can be seen (as the bright red patches) "floating" in the bladed anhydrite.

Bottom Photomicrograph

The same field of view is shown here under Pl at the same magnification. Note that there are only faint hints of the dolomite-filled solution mold after the phylloid-algal plate from bottom center to right center. In addition, the plane-transmitted lighting does not show any internal growth zonation of the replacement dolomite in the left half of this view. However, the bladed lathes of replacement anhydrite are visible along the right hand margin of this photomicrograph.

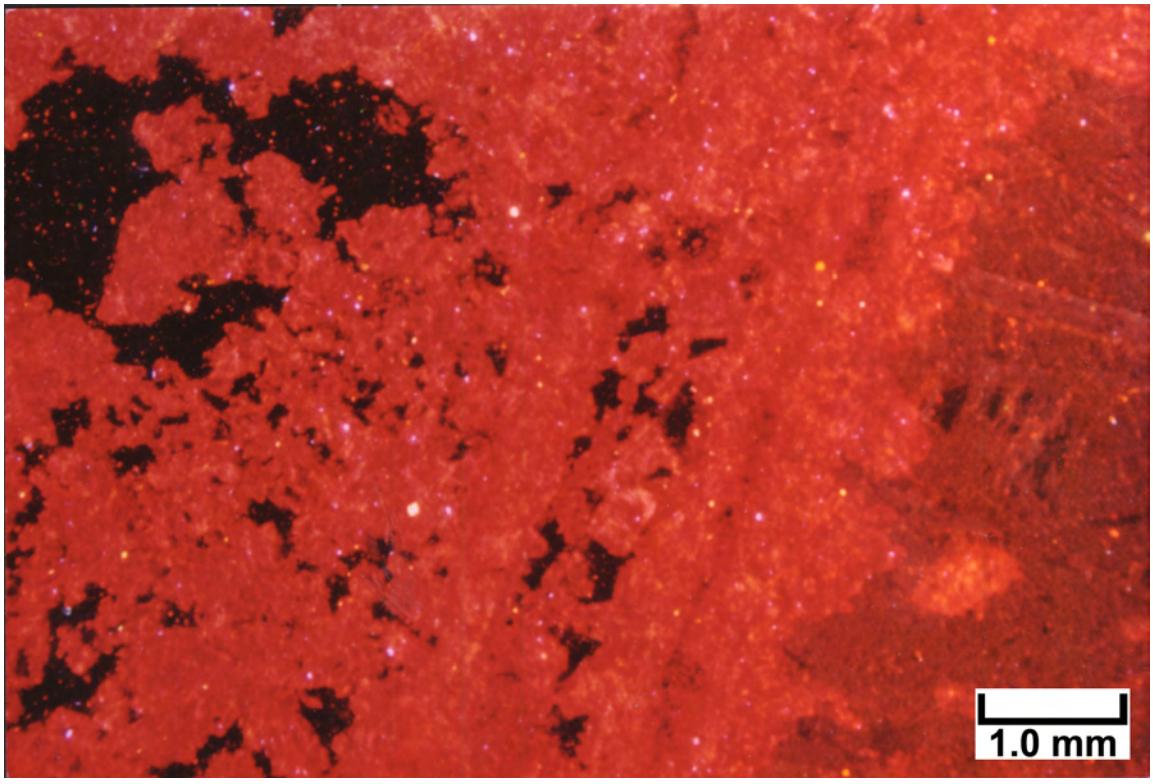
1.0 mm

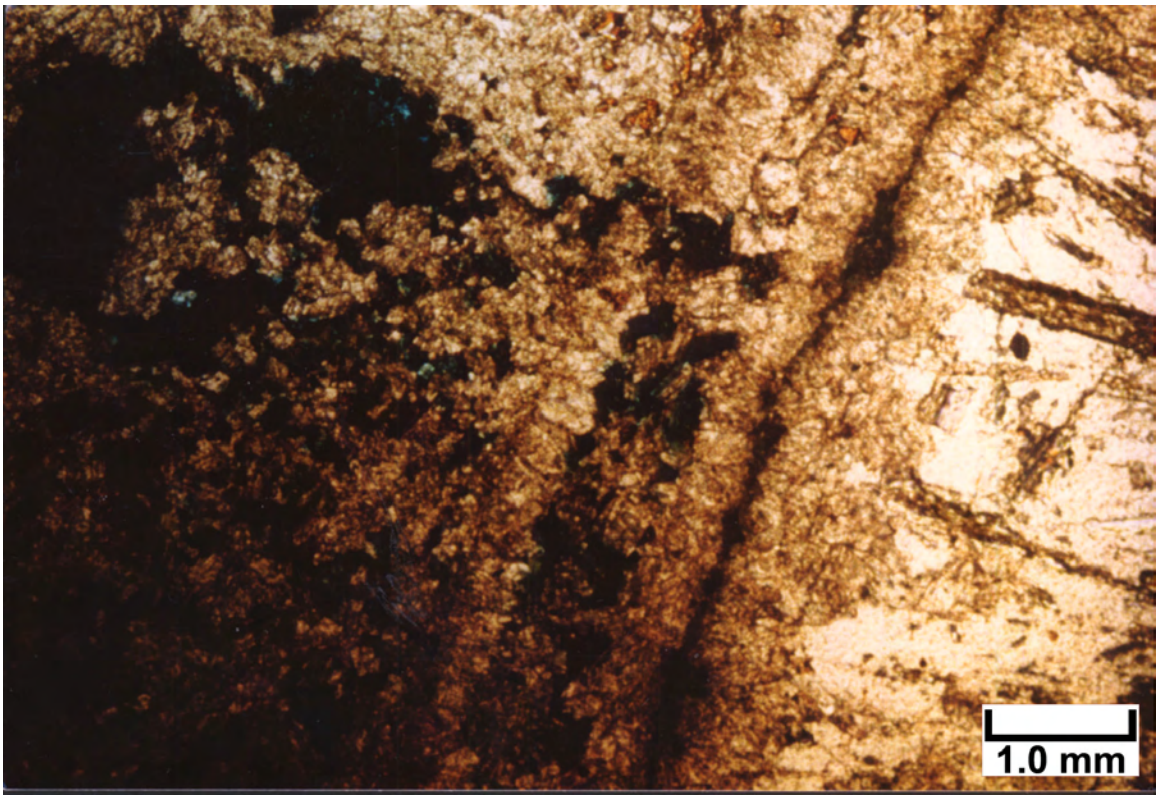
1.0 mm

6312 feet

Top Photomicrograph

This CL overview shows a completely dolomitized carbonate sediment that was well-cemented prior to dolomitization. Note that the darker red patterns show ghosts or remnants of the original carbonate sediment grains (mostly peloids and fragmented skeletal debris). The brighter, orangish red areas show the original areas of carbonate cement. The black patches represent open pores, which are a combination of remnant primary (uncemented) pores and possibly small solution cavities. The yellow, white, and blue specks disseminated throughout this dolomite are mostly silt-sized detrital siliciclastic grains (mostly quartz and feldspar) that were probably delivered to this sediment by eolian processes.

Bottom Photomicrograph

The same field of view is shown here under Pl at the same magnification. Except for the very dark blue open pores, it is very difficult to distinguish carbonate grains from cement in this microcrystalline dolomite without the use of CL.

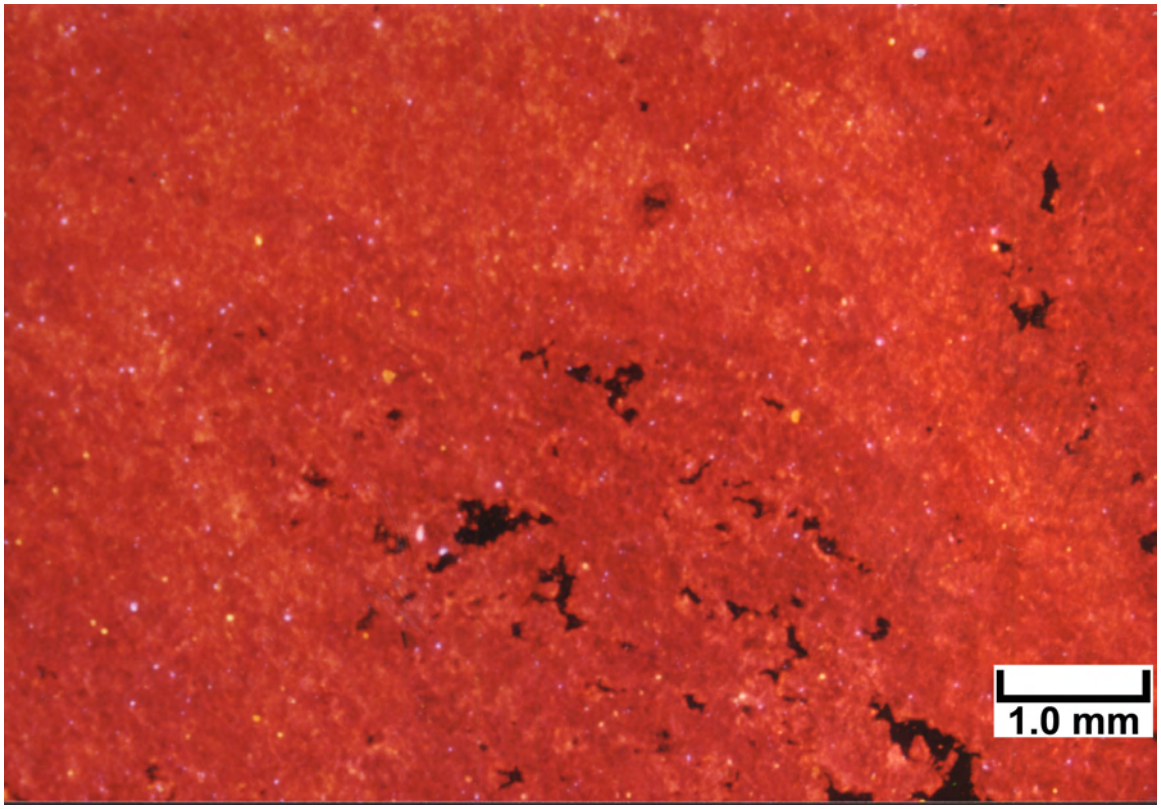
1.0 mm

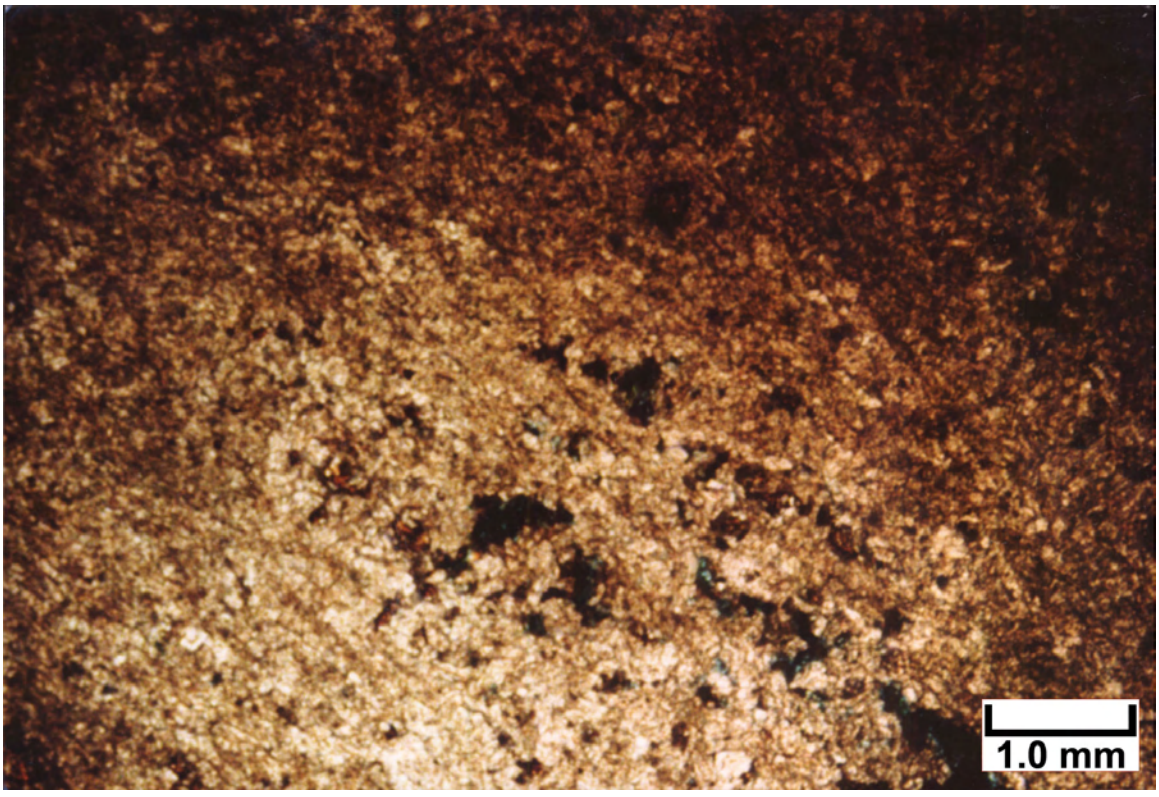
1.0 mm

6312 feet

Top Photomicrograph

Cathodoluminescence imaging of a completely dolomitized phylloid-algal bafflestone nicely shows the distinction between original carbonate grains (in dull red) versus early cements (in bright orangish red). Note the two orientations of microfracture swarms which trend from top to bottom and from left to right in this view. Many of these microfractures can be seen as the dark gray to black curvilinear lines. It is possible that some of these open microfractures may have originated from dissolution along microstylolites.

Bottom Photomicrograph

The same field of view is shown here under Pl at the same magnification. Note that it is difficult to determine original carbonate grains from early carbonate cements in this transmitted plane-light view. Open pores can be seen as the blue epoxy-filled areas. Although it is possible to see some intercepting microfractures here, the CL view above nicely shows additional microfractures.

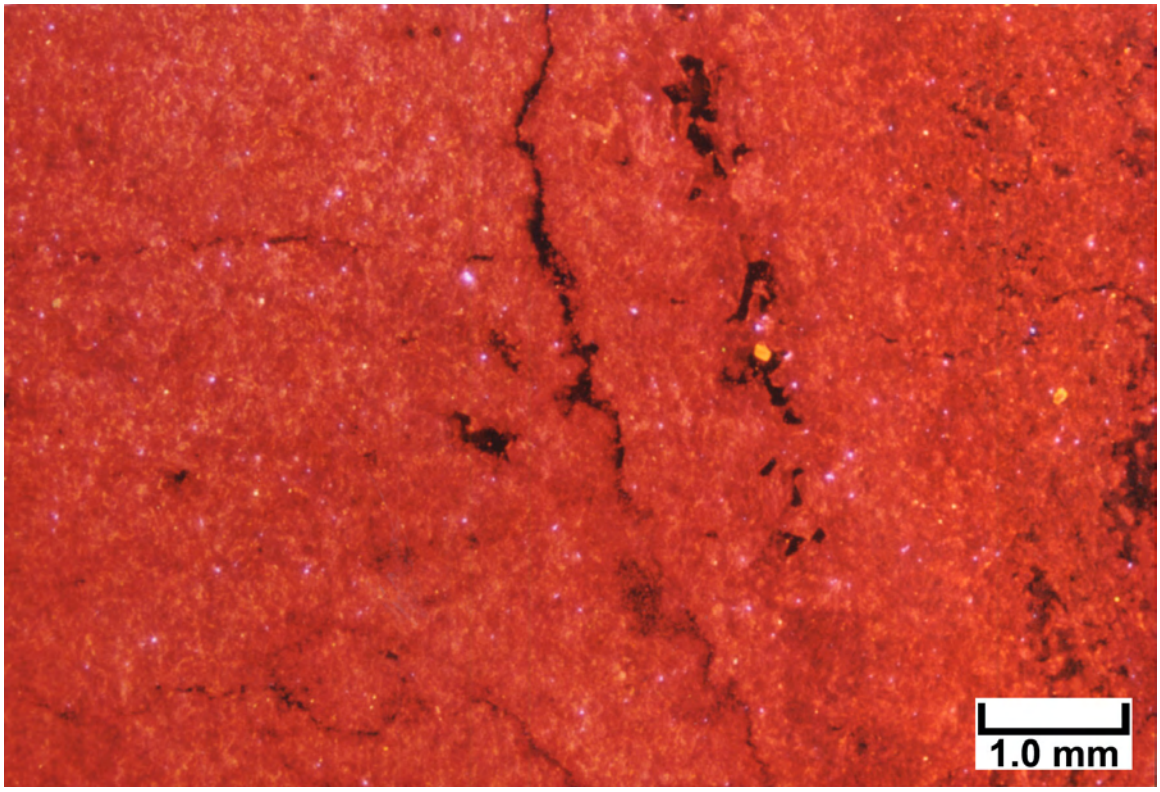
1.0 mm

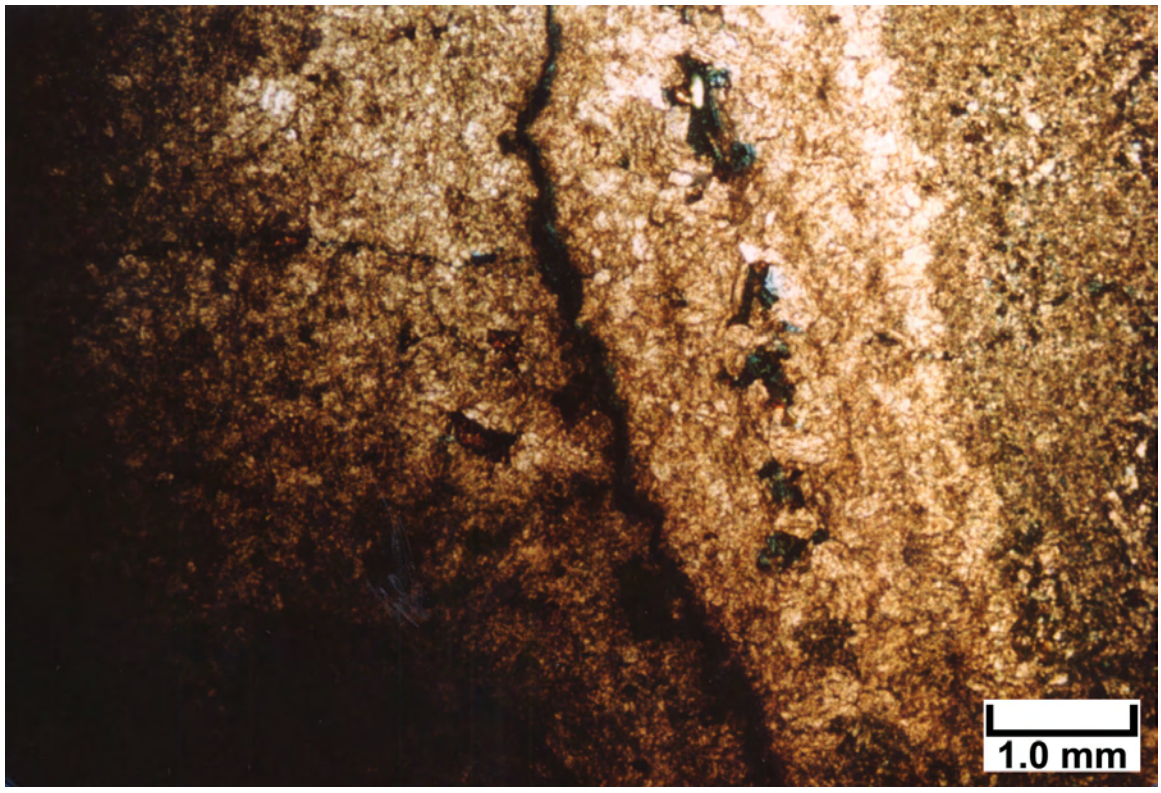
1.0 mm

BUG NO. 10 WELL,
BUG FIELD

6327.5 feet

Top Photomicrograph

Cathodoluminescence imaging clearly shows some of the distinctive fabric elements within a completely dolomitized, phylloid-algal/skeletal, grain-rich sediment. Note the elongate blades of poorly preserved phylloid-algal plates from bottom center to upper right in this micrograph. Within these blades are preserved remnants of skeletal materials in bright red, and cements in dull reddish gray. For the most part, dolomitized skeletal grains, or their remnants, appear as bright red luminescent areas with clear skeletal shapes. Some of the grains easily visible in this field of view are rounded crinoids with their distinctive circular cores and single crystal, red luminescent rims. Early cements (prior to dolomitization) are very dull red. Porous microdolomites dominate the left quarter of this micrograph. Note also the remnants of dolomitized bladed cements and micro-box-work dolomite fabrics visible in the upper left center of this view. The black areas throughout this field of view are open pores.

Bottom Photomicrograph

The same field of view is shown here under combined Pl and CL (that is, a double exposed image) at the same magnification. In this view, remnants of bright red luminescence show through the coarse and fine dolomite crystal patterns. The blue and black areas of this slide consist of open pores.

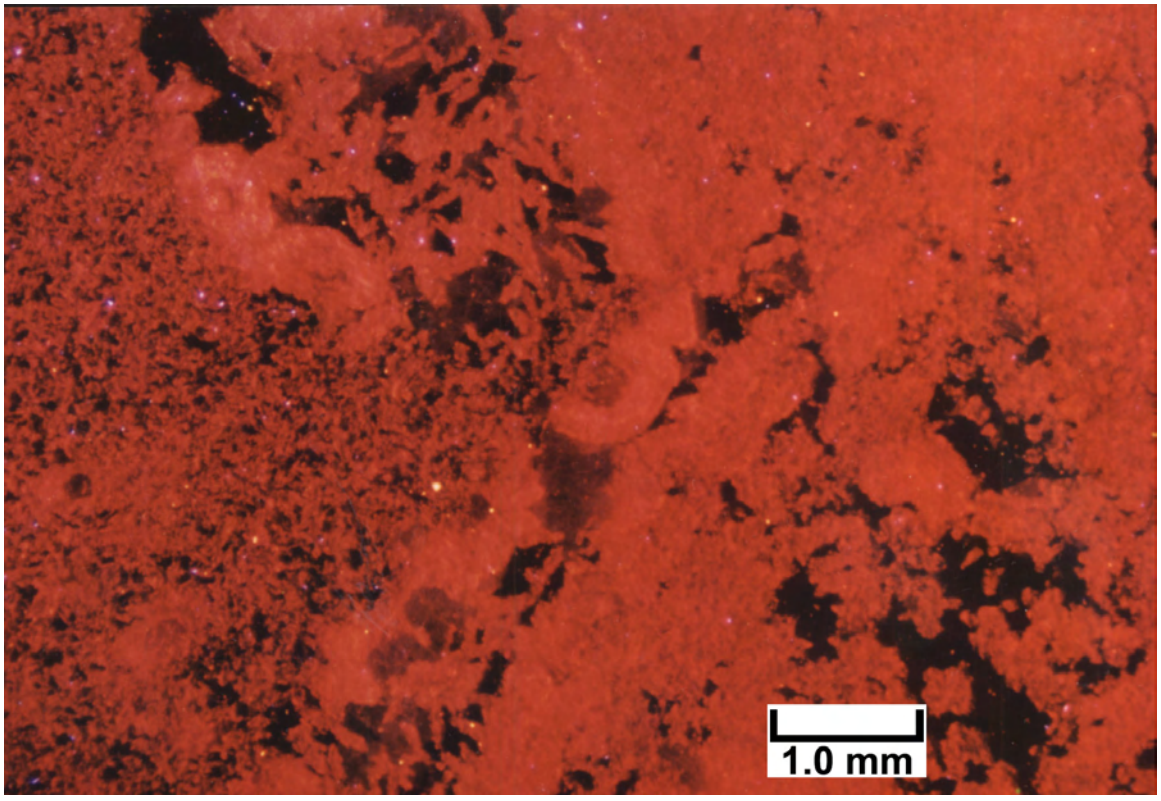
1.0 mm

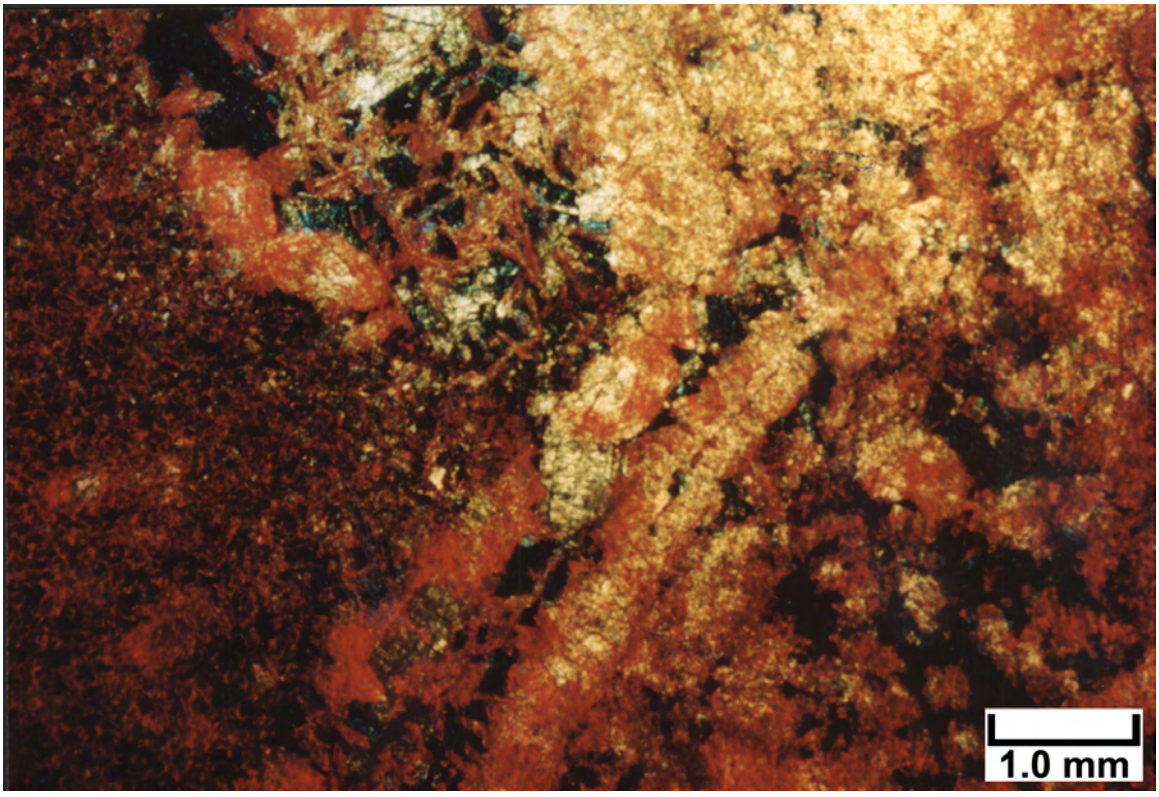
1.0 mm

6327.5 feet

Top Photomicrograph

Cathodoluminescence imaging nicely shows remnants of phylloid-algal plates (from upper to lower center) that are lined with bladed cements exhibiting bright and dull bands. Other features within this completely dolomitized mound fabric can be seen within both the dolomitized sediments in the upper left corner and the zoned dolomite cements within the megascopic and microscopic porosity patches (in black) throughout this micrograph. Cathodoluminescence in this image is very effective in distinguishing the pore boundaries from the dolomite matrix crystal boundaries.

Bottom Photomicrograph

The same field of view is shown here under Pl at the same magnification. Note that there is relatively little detail preserved within this dolomite other than vague patches of dark brown and clear crystals. Details of different zoned and replacement dolomite crystals can be seen more clearly in the CL view above. The blue areas within this view are open pores impregnated with blue epoxy.

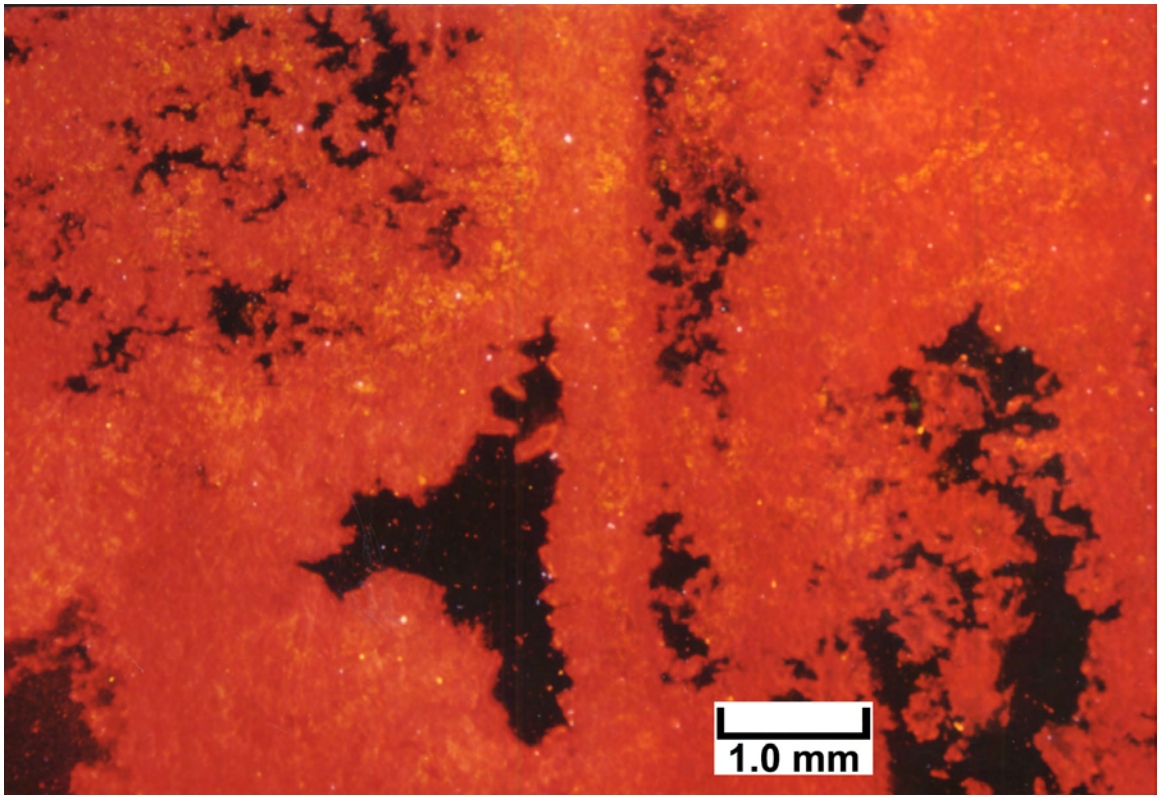
1.0 mm

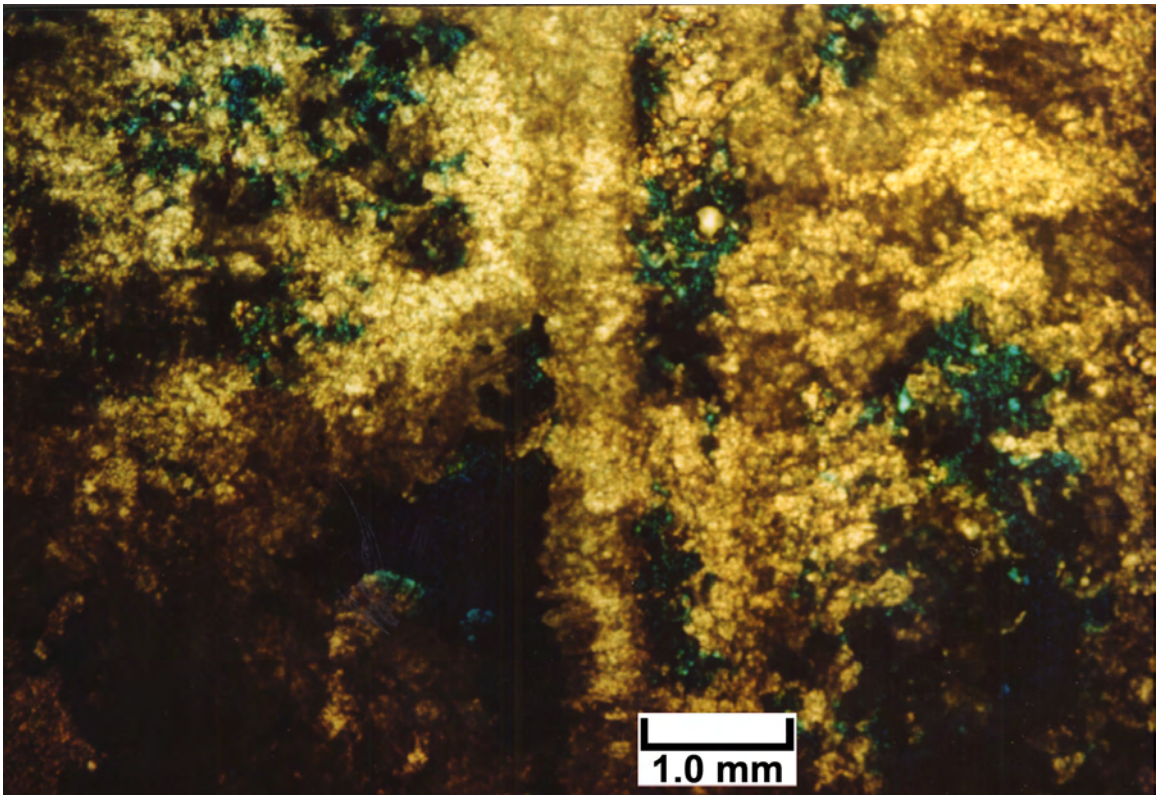
1.0 mm

6327.5 feet

Top Photomicrograph

This CL overview very nicely shows the distribution of completely dolomitized sediment in various shades of red versus open pores in the black areas. It is easy to see the well-connected macro- and micro-pore links. Within this view, it is difficult to distinguish individual carbonate grains from cements. But in general, the dull, intense reds conform to dolomitized carbonate grains and the brighter, orangish red areas are remnants of dolomitized early cements. Note that this sample displays a highly brecciated character, followed by some dissolution and corrosion of grains and cements.

Bottom Photomicrograph

The same field of view is shown here under Pl at the same magnification. Despite the areas of blue and black within this view, the ability to clearly identify pores versus dolomitized matrix is difficult. Black bitumen linings of most pores make this identification difficult. However, better resolution of dolomite matrix versus open pores can be seen in the CL view above.

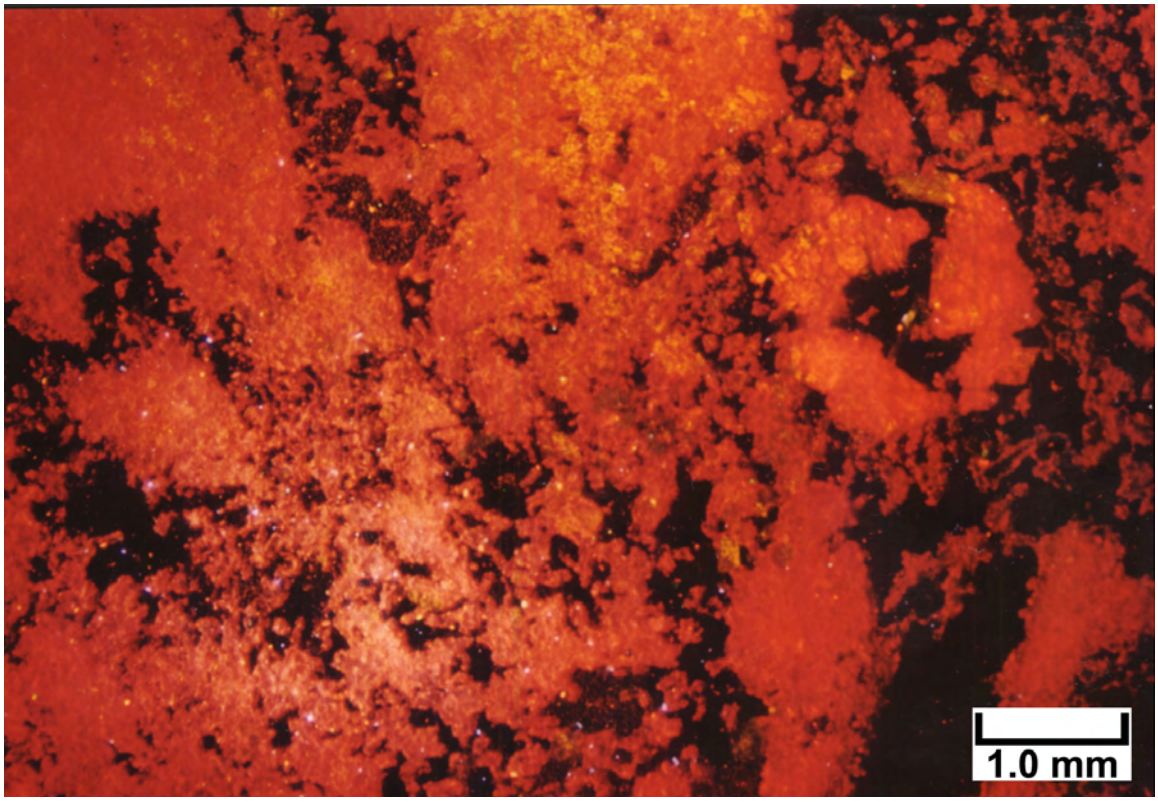
1.0 mm

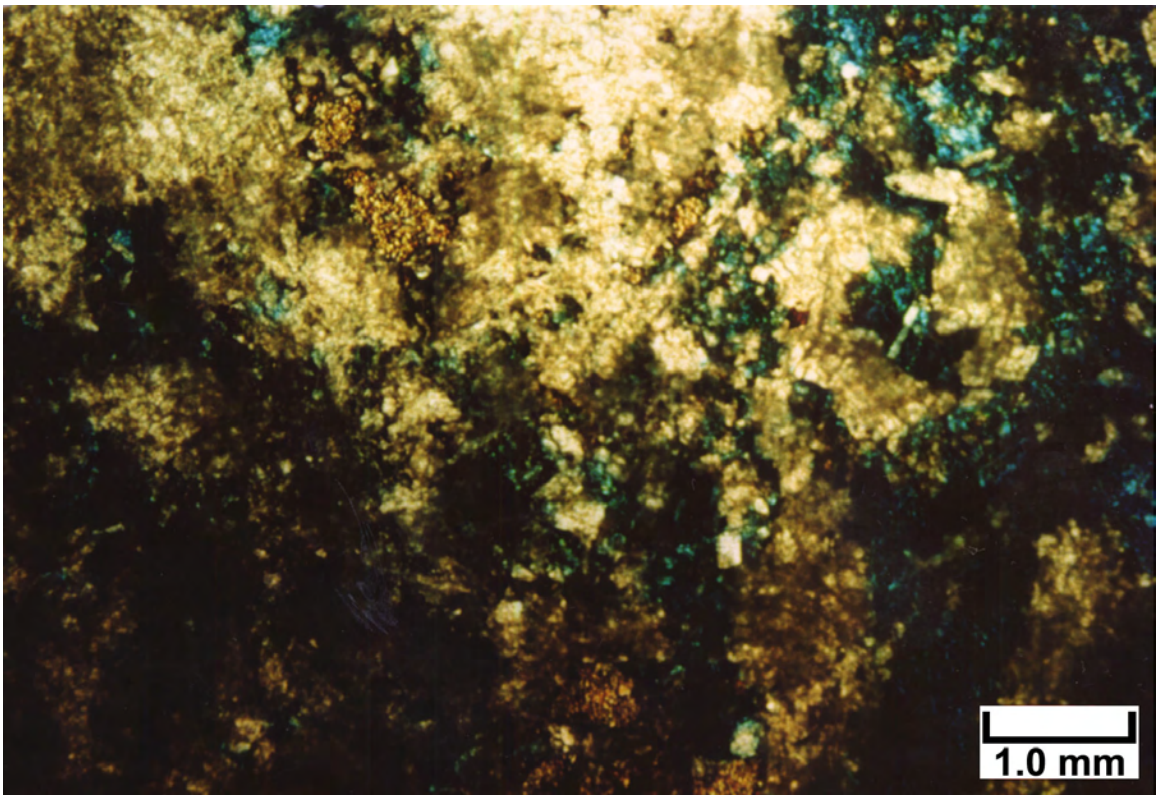
1.0 mm

BUG NO. 13 WELL,
BUG FIELD

5930.6 feet

Top Photomicrograph

This CL view is from a sample of pisolites and coated-grain aggregates. Note that it is possible to see the carbonate-grain outlines (in uniformly dull red) versus early carbonate cements (in orangish red). Late-stage, dolomitized, spar crystals can be seen in the dull-gray patches in the lowermost and uppermost center of this view. The black (non-luminescent) areas clearly image the open pores and microfractures.

Bottom Photomicrograph

The same field of view is shown here under Pl at the same magnification. In this view, it is possible to see the large coated grain aggregates (pisolites and possible grapestones). However, Pl viewing does not show the individual carbonate grains that compose the larger grain aggregates as well as the CL imaging.

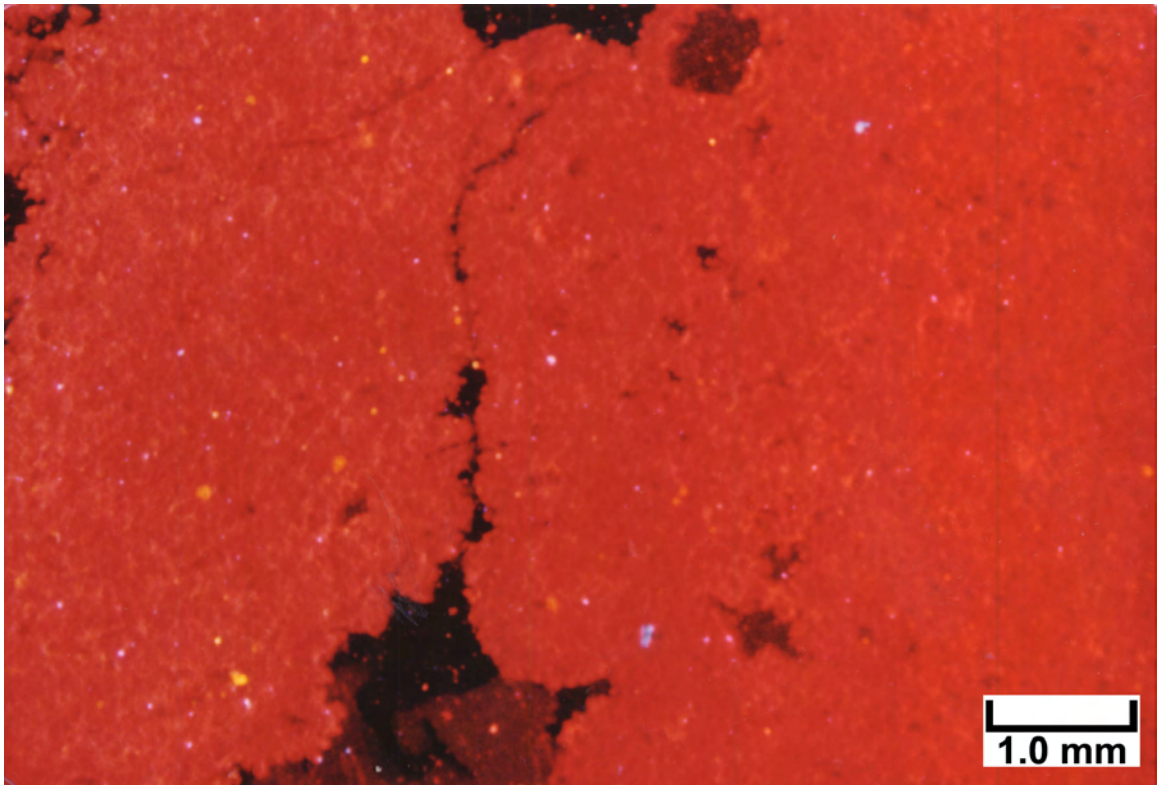
1.0 mm

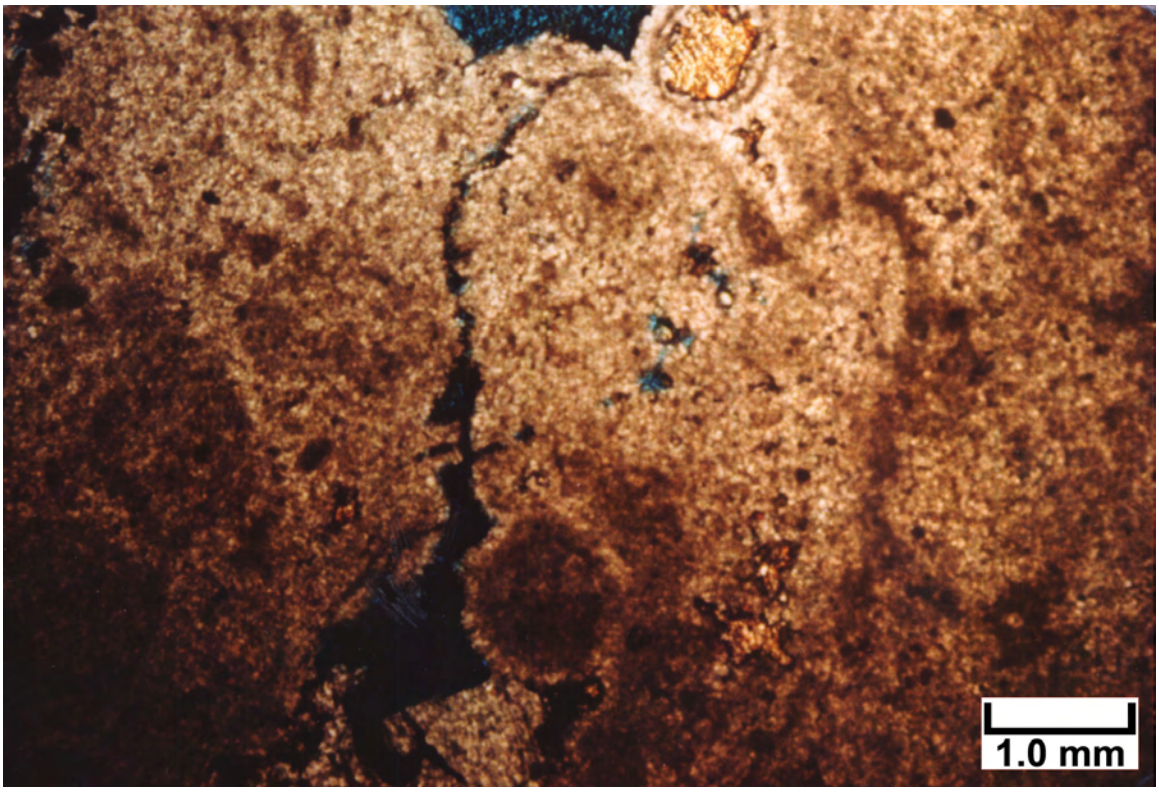
1.0 mm

5930.6 feet

Top Photomicrograph

Cathodoluminescence imaging of internal muddy sediment between coated-grain aggregates and brecciated phylloid-algal fabrics is shown here. The bright blue specks consist of quartz silt grains that were probably delivered to this internal sediment by eolian processes. Individual dolomitized carbonate grains can be resolved by the shapes associated with bright-red and dull-red color patterns. Note that there is a distinct pelleted appearance to the dense mud portions of this view (especially in the right half of this micrograph). Most of the orangish red areas consist of pre-dolomitization cements. The black patches are associated with open pores and microfractures.

Bottom Photomicrograph

The same field of view is shown here under Pl at the same magnification. Only vague outlines of possible carbonate grains and dense, dark colored carbonate muds can be seen here. Dolomitization of this internal sediment has destroyed most of the original fabric definition. Without CL, the detrital quartz silt grains and many of the sand-sized carbonate grains would not be identifiable.

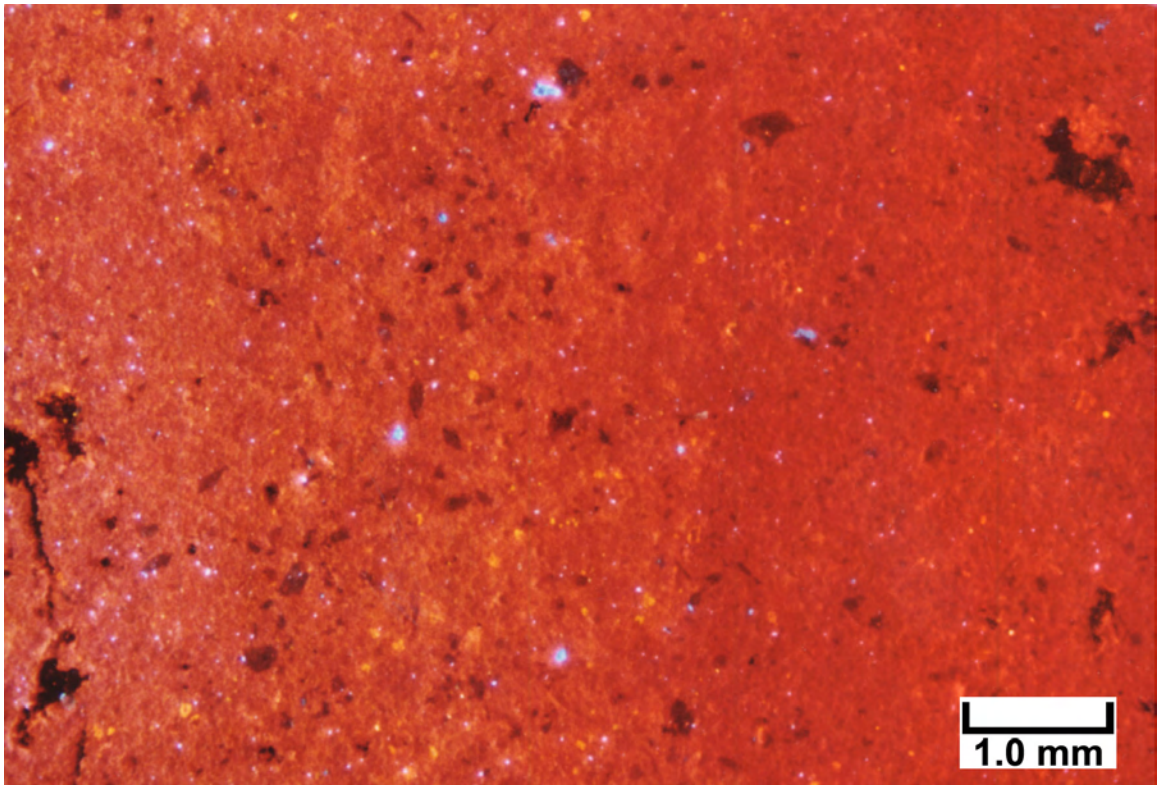
1.0 mm

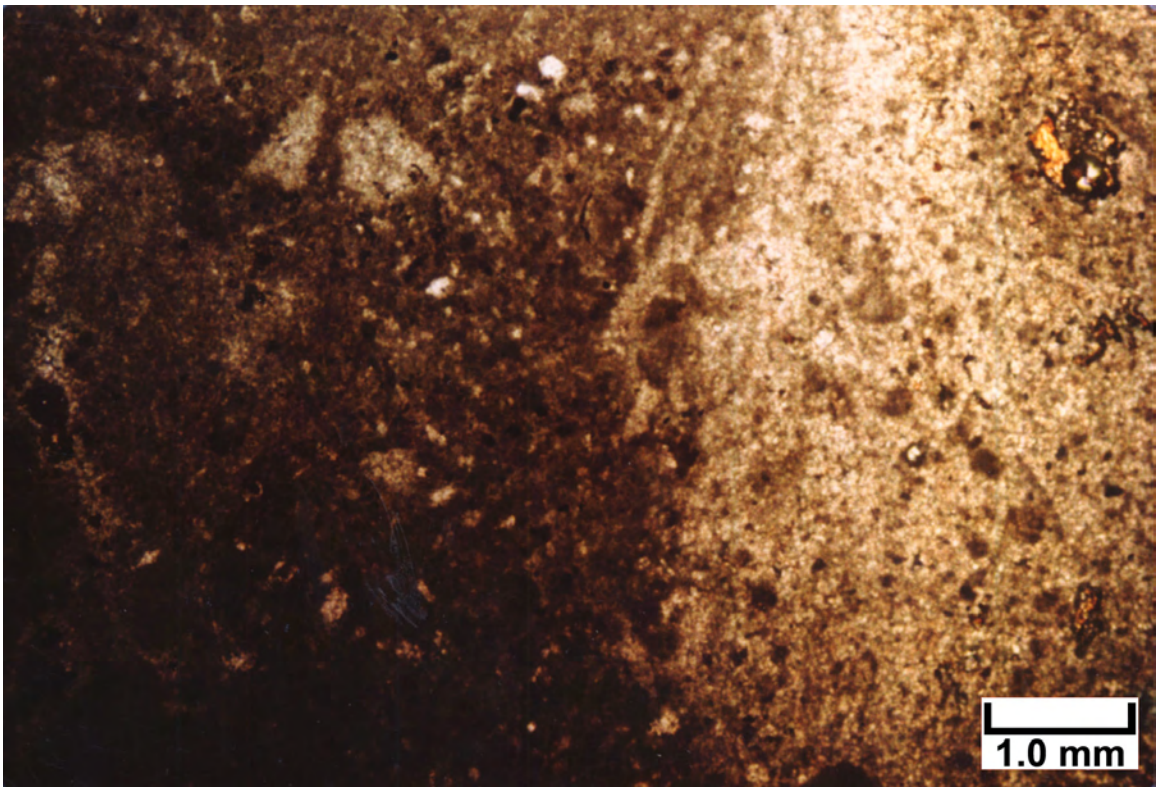
1.0 mm

BUG NO. 16 WELL,
BUG FIELD

6300.5 feet

Top Photomicrograph

Cathodoluminescence of an area displaying micro-box-work dolomite and early fibrous marine cements is imaged here. Note the patterns of dull red, bright red, and orangish red throughout this dense, tight dolomite. Most of the original carbonate fabric associated with carbonate sediment and early marine cements can be seen in the dull and bright red patterns. The orangish red areas represent later dolomite cement growth bands. In some areas of this view (especially in the left third of the image), there are dolomite crystals that have developed a clear rhombic shape. The black areas clearly define open pores associated with dissolution as well as the development of intercrystalline porosity.

Bottom Photomicrograph

The same field of view is shown here under Pl at the same magnification. Only the outlines of larger dolomite crystals are visible here. Cathodoluminescence imaging, as shown above, brings out the internal original fabric versus later dolomite growth zones much more clearly. The blue patches are open pores lined with black bitumen. The presence of bitumen makes it difficult to clearly discern the outlines of dolomite matrix versus open pores under Pl. Cathodoluminescence (above) images the pore/rock boundaries very well.

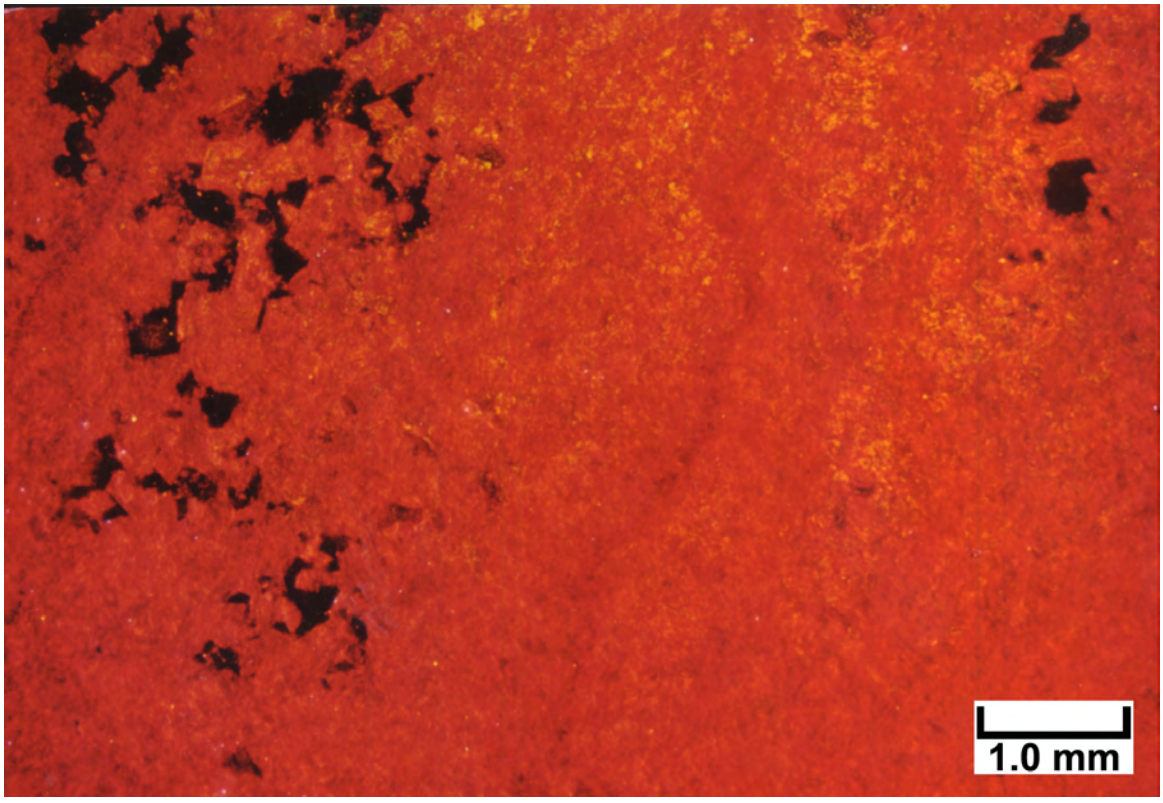
1.0 mm

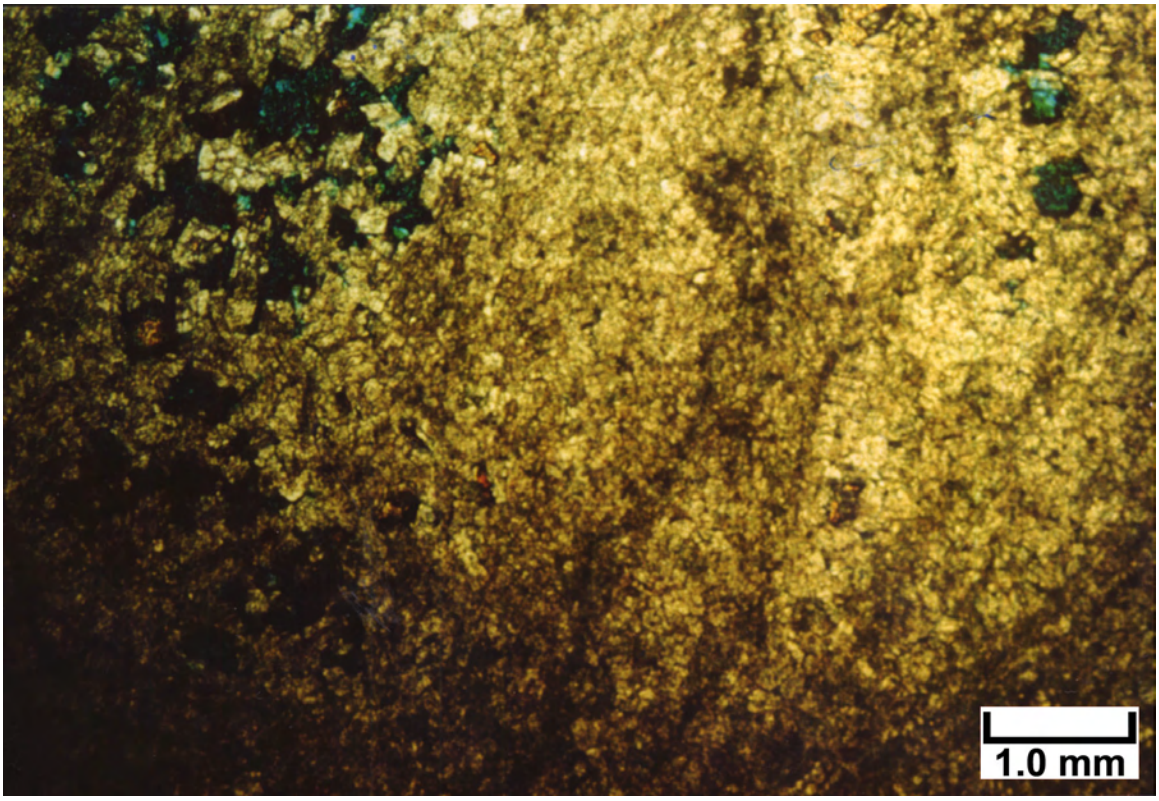
1.0 mm